



An Archean megacaldera complex: The Blake River Group, Abitibi greenstone belt

V. Pearson^a, R. Daigneault^{b,*}

^a CONSOREM – Consortium de recherche en exploration minérale, 555 Boul. de l'Université, Chicoutimi, Canada G7H 2B1

^b Centre d'études sur les Ressources minérales (CERM) – Université du Québec à Chicoutimi, 555 Boul. de l'Université, Chicoutimi, Canada G7H 2B1

ARTICLE INFO

Article history:

Received 3 July 2007

Received in revised form 31 March 2008

Accepted 31 March 2008

Keywords:

Caldera
VMS deposits
Greenstone belt
Archean
Blake River Group
Abitibi greenstone belt

ABSTRACT

The Archean Blake River Group of the southern Abitibi greenstone belt is defined as a subaqueous megacaldera. Compelling evidence include: (1) a radial and concentric organization of synvolcanic mafic to intermediate dykes, (2) an overall dome geometry defined by the volcanic strata, (3) a peripheral distribution of subaqueous volcanoclastic units, (4) a zonal distribution of carbonate alteration, and (5) a distinct annular synvolcanic inner and outer ring fault pattern. Three caldera-forming events have been identified: (1) the early Misema caldera, (2) the New Senator caldera, and (3) the well-known Noranda caldera. The multi-vent BRG mafic volcanic complex, developed on a monotonous sequence of tholeiitic basalts, forming a submarine plain, and experienced a first major collapse that created the giant Misema Caldera (80 km in diameter). An endogenic dyke swarm intruded the synvolcanic fractures and an underlying magma chamber developed. Major volcanoclastic units were generated by local volcanic centers and summit calderas formed along the outer and inner ring faults. This fault system was used as a conduit for CO₂-rich hydrothermal activity. Renewed volcanic activity was associated with a resurgent central dome inside the Misema Caldera. This second collapse event created the 35 km by 14 km NW-trending New Senator Caldera. This caldera was produced by multi-step sagging after the underlying magmatic chamber migrated to the SE and formed the Flavrian-Powel Plutons. The final collapse resulted in the formation of the Noranda Caldera that generated a well-developed 070°-trending fracture pattern associated with several VMS deposits. The multiple-caldera setting provides an effective model to explain the presence of VMS mineralization along the synvolcanic fractures associated with the three collapse episodes. However, the importance of the New Senator Caldera fracture pattern is emphasized because of its role in the positioning of the giant Horne Mine deposit.

© 2008 Elsevier B.V. All rights reserved.

1. Introduction

Calderas are subcircular collapse structures related to overpressure or underpressure conditions of the underlying magma chamber (Lipman, 1997; Gudmundsson, 1998a). Recognition in modern subaerial settings, such as the Toba (Chesner et al., 1991), Taupo (Charlier et al., 2005) and Valles calderas (Self et al., 1996), is facilitated by their 3D geomorphology and preserved volcanic deposits. In contrast, submarine calderas are problematic because of limited access. Topographic and geophysical surveys are used in subaerial settings, whereas bathymetric maps reveal the geometry of their subaqueous counterparts (Fiske et al., 1998, 2001). Subaqueous silicic calderas are recognized as first order sites for volcanogenic massive sulphides (VMS; Ohmoto, 1978, 1996; Stix et al., 2003; Franklin et al., 2005), and hence their importance for exploration.

Archean greenstone belts are dominated by submarine sequences and numerous subaqueous calderas have been identified based on lithofacies distribution and regional mapping (Morton et al., 1991; Gibson et al., 1999; Mueller et al., 2004, 2008). Although regional ductile deformation events manifested by folds, faults and shear zones make it difficult to reconstruct the geometry of the volcanic architecture, steeply dipping units in plan view can be interpreted as a section across a caldera (Mueller and Mortensen, 2002; Hudak et al., 2003; Lafrance et al., 2003).

The initial model for the Blake River Group (BRG) in the Archean Abitibi greenstone belt was of a mafic, basalt-dominated base (Goodwin, 1977) upon which a felsic complex developed (de Rosen-Spence, 1976; Dimroth and Lichtblau, 1979). This study presents a fundamental re-interpretation of the Blake River Group based on the pattern of mafic to intermediate dykes and sills, the synvolcanic fracture systems, and the distribution of volcanoclastic deposits. The Blake River megacaldera complex (BRMCC) with a diameter of 80–90 km is equivalent to the dimension of the Olympus Mons summit caldera on Mars. Despite some deforma-

* Corresponding author. Tel.: +1 418 545 5011x5634; fax: +1 418 545 5011x5634.
E-mail address: rdaignea@uqac.ca (R. Daigneault).

tion, the BRMCC has preserved a geometry and features typical of both overlapping (Las Cañadas Caldera, Tenerife; Carracedo et al., 2007) and nested calderas (Campi Flegrei field, Naples; Mueller et al., 2008). This new interpretation has significant implications for understanding Archean tectonic evolution and defining new exploration targets for volcanogenic massive sulphides in the BRG.

2. Geological setting

The 3000-km² BRG is characterized by a 2706(?)–2696 Ma volcanic sequence (Corfu, 1993; Mortensen, 1993a,b; Mueller et al., 2007) belonging to the southern volcanic zone of the Abitibi Subprovince (SVZ; Chown et al., 1992; Fig. 1). The 4–7 km-thick BRG succession is composed of mafic volcanic rocks with several felsic volcanic centers (Baragar, 1968; Jolly, 1980; Dimroth et al., 1982; Jensen, 1981; Hannington et al., 2003). This well-preserved, low-grade metamorphic, volcanic succession (Jolly, 1978; Gélinas et al., 1984) hosts 33 volcanogenic massive sulphide (VMS) deposits totalling 125 Mt with the 54 Mt (150 total) giant Horne Mine deposit as the major producer (Fig. 2).

The BRG was subdivided into Misema and Noranda subgroups (Goodwin, 1977; Péloquin, 2000, Fig. 2). The basal Misema Subgroup is dominated by tholeiitic and calc-alkaline mafic volcanic rocks with local mafic and felsic centers (Fig. 2) such as Clifford and Ben Nevis (Gélinas et al., 1977; Jensen, 1981; Ayer et al., 2005). A mafic variolitic volcanic unit along the margin of the BRG is a marker unit at the base of the group (Dimroth et al., 1982). The tholeiitic to calc-alkaline overlying Noranda Subgroup is distinctly bimodal, with felsic volcanic rocks accounting for up to 40% of the subgroup by volume (Gélinas et al., 1977, 1984).

The Misema Subgroup is interpreted to be derived from the partial melting of a mantle-source, fractionating garnet and amphibole (Baragar, 1968; Goodwin and Smith, 1980). The source of the Noranda Subgroup is recognized to be a garnet-free high level magma with different degrees of assimilation and fractional crystallization, implying ensialic to ensimatic components (Ludden et al., 1982; Capdevilla et al., 1982; Hart et al., 2004).

2.1. The Noranda Caldera

The Noranda Caldera (NC) was recognized by de Rosen-Spence (1976) and Lichtblau and Dimroth (1980) and studied in detail by Gibson (1989), who referred to it as the Noranda cauldron. The NC is oval-shaped, measures 15 km by 20 km, and lies between synvolcanic faults: the Hunter Creek Fault (HuCF) to the north, the Horne Creek Fault (HoCF) to the south and the Dufresnoy Fault (DF) to the east (Fig. 2). Subsidence reached a maximum of 1200 m along the southern margin (Gibson, 1989), which suggests an asymmetric trapdoor structure (e.g. Lipman, 1997). Numerous felsic units of the Noranda Subgroup are associated with the caldera (unit 3 in Fig. 2, de Rosen-Spence, 1976; Gibson, 1989), whereas other units are interpreted to be pre- or post-caldera (Gibson, 1989). Spatially associated with these collapse structures is the 2700 ± 2 Ma composite tonalitic to trondhjemitic synvolcanic Flavrian Pluton (Mortensen, 1993a,b; Galley and van Breemen, 2002). Within the caldera, numerous ENE-trending synvolcanic faults served as hydrothermal fluid conduits to generate VMS deposits (Gibson, 1989). The volcanic architecture of the substratum around and underneath the Noranda Caldera remains unknown.

2.2. Geochronology

Available geochronological data indicate that the BRG felsic volcanic activity is bracketed between 2694 ± 2 and 2701 ± 1 Ma

(Fig. 2). The climax around 2698 Ma corresponds to the median age for the synvolcanic felsic intrusive rocks. Felsic volcanism of Misema and Noranda subgroups is considered coeval as radiometric determinations do not show a spatial distribution pattern.

2.3. Deformation

Archean terranes are generally affected by several deformational events so that folding and faulting need to be carefully addressed to make paleogeographic reconstructions (see Daigneault et al., 2004). The present surface geometry of the BRG defines a lens-shaped unit extending 125 km by 40 km with a relatively low-strain domain in the central part, in which subhorizontal units are recognized. The strain level increases progressively towards the margins of the BRG, as expressed by a subvertical dip of the volcanic units and the appearance of ductile planar fabrics. The ductile deformation becomes more developed near the two major fault zones limiting the BRG, the Destor-Porcupine-Manneville Fault Zone (DPMFZ) to the north and the Cadillac-Larder Lake Fault Zone (CLLFZ) to the south (Fig. 2). The SE-trending Parfouru Fault Zone (PFZ) is also recognized at the eastern margin of the BRG. Although the effects of ductile deformation can be discerned within the BRG, internal primary characteristics within the overall architecture were nonetheless preserved.

3. The Blake River Megacaldera Complex and Misema Caldera

The Blake River Megacaldera Complex (BRMCC) is defined as a multi-stage collapse structure that occupies most of the present BRG surface. Several arguments support a megacaldera complex and include: (1) the mafic-intermediate dyke swarm pattern (Figs. 3 and 4), (2) the overall domal geometry (Fig. 5), (3) the fault pattern (Fig. 6), (4) the distribution of volcanoclastic rocks (Fig. 7), and (5) the distribution pattern of carbonate-rich hydrothermal alteration (Fig. 8). These components collectively support the definition of the giant Misema Caldera (MC) as well as the subsequent New Senator (NSC) and Noranda (NC) calderas.

3.1. Ring and radial dyke patterns

The distribution of the BRG mafic to intermediate dyke swarms was determined by detailed mapping and integrating the company databases (e.g. Dimroth et al., 1985; Gibson, 1989; MRNFP, 2005) (Fig. 3). The gabbroic and dioritic dykes have chemical compositions and magnetic susceptibilities similar to those of their host volcanic rocks (Jensen, 1981). Few radiometric determinations have been done on the mafic dykes, but the 2707 Ma Aldermac quartz- and feldspar-phyric gabbro (Vaillancourt, 1996) and the recently dated 2703 Ma gabbro in the Clericy area (Mueller et al., 2007) indicate a synvolcanic nature.

The general dyke pattern for the whole BRG displays a consistent concentric and radial organization (Fig. 3). The concentric pattern mainly follows the shape of the BRG with a virtual center point occupied by the Flavrian Pluton, a pattern followed also by the distribution of the felsic rocks units (Figs. 2 and 3). The overall shape becomes flattened near the major Cadillac-Larder Lake Fault Zone that marks the southern BRG boundary.

3.1.1. Ovoid dyke patterns

Careful examination of dyke distribution reveals the presence of km-scale concentric and radial dyke patterns, particularly in the northern part of the BRG (Fig. 3). Ovoid patterns are commonly elongated (1:2 ratio), have a restricted extent (5–10 km in the long axis), and in several cases occur around a felsic pluton. These ovoid

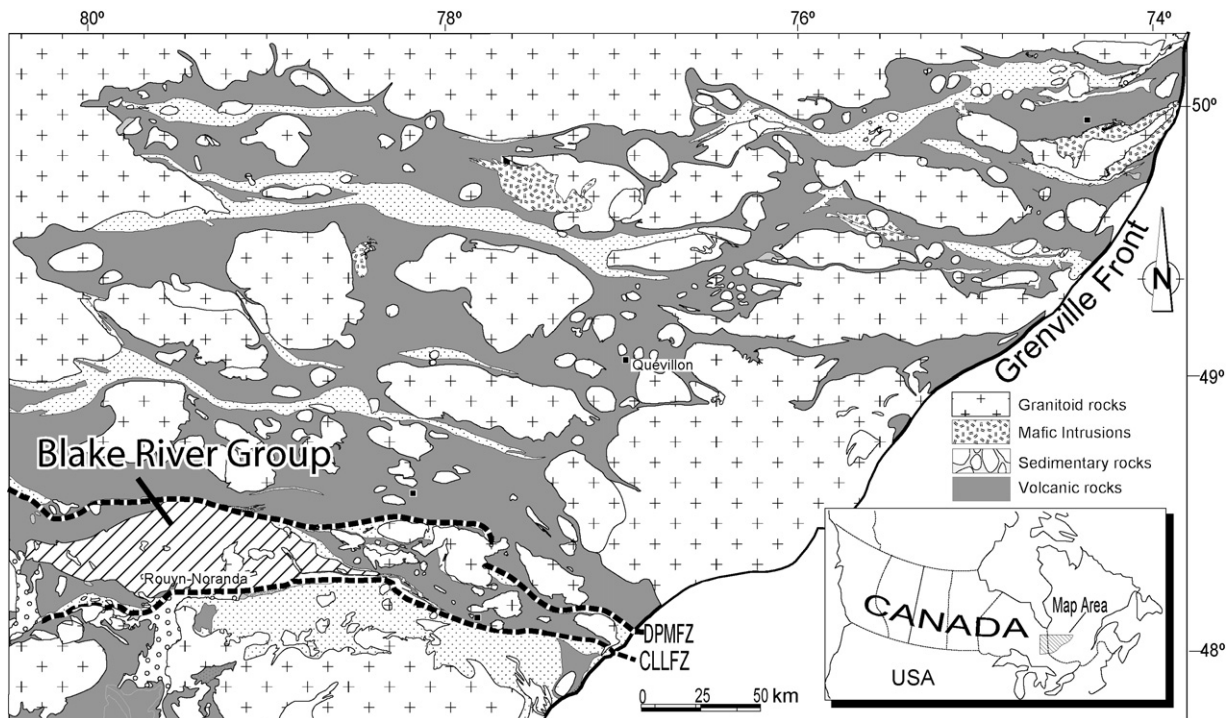


Fig. 1. Location of the Blake River Group in the Abitibi Subprovince (modified from Daigneault et al., 2004). DPMFZ = Destor Porcupine Manneville Fault Zone, CLLFZ = Cadillac Larder Lake Fault Zone.

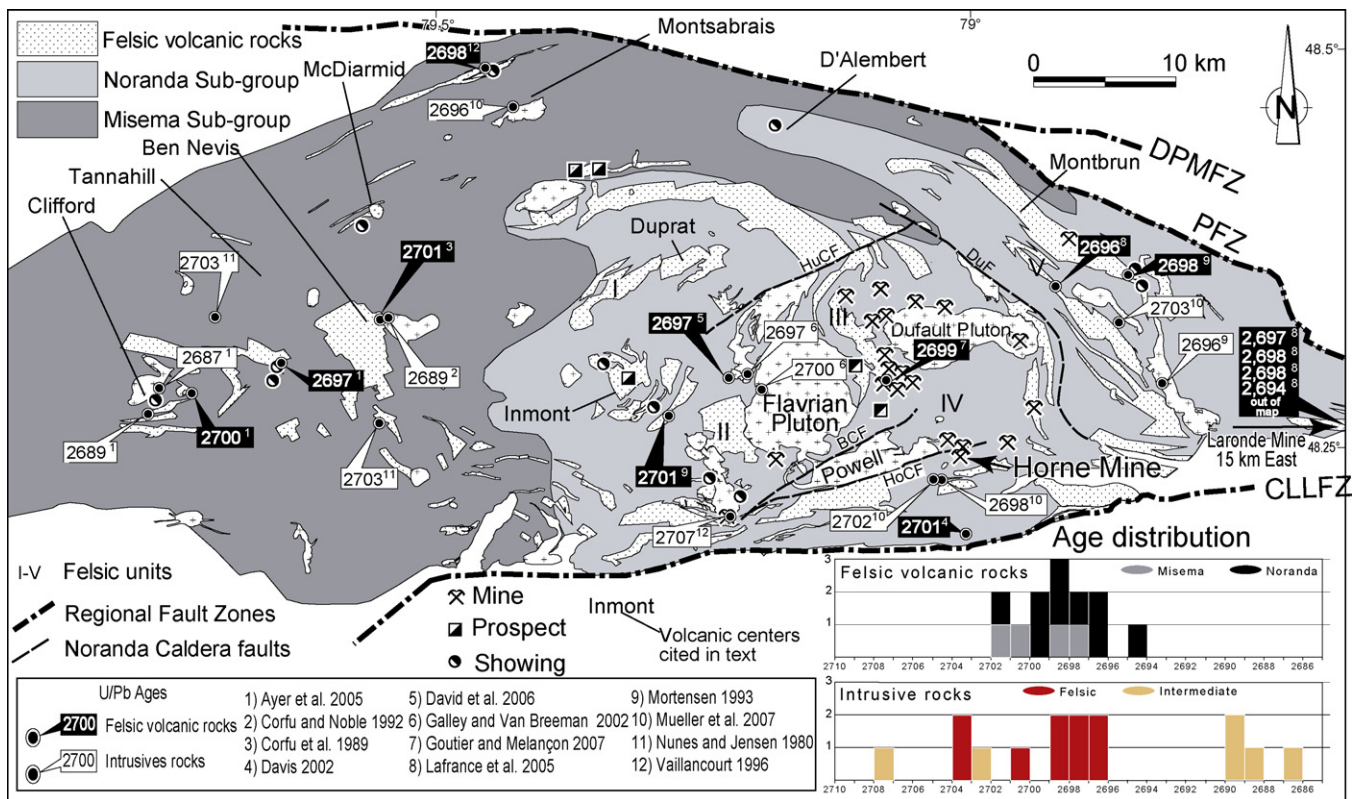


Fig. 2. Map showing the relevant features of the Blake River Group and the distribution of the two subgroups (Misema and Noranda) and felsic volcanism. Roman numerals refer to felsic units of the Noranda Subgroup (Gibson and Watkinson, 1990). The Hunter Creek Fault (HuCF), Horne Creek Fault (HoCF) and Dufresnoy Fault (DuF) are boundary faults around the Noranda Caldera (de Rosen-Spence, 1976; Gibson and Watkinson, 1990). DPMFZ = Destor-Porcupine-Manneville Fault Zone, CLLFZ = Cadillac-Larder Lake Fault Zone, PFZ = Parfouru Fault Zone, BCF = Beauchastel Creek Fault.

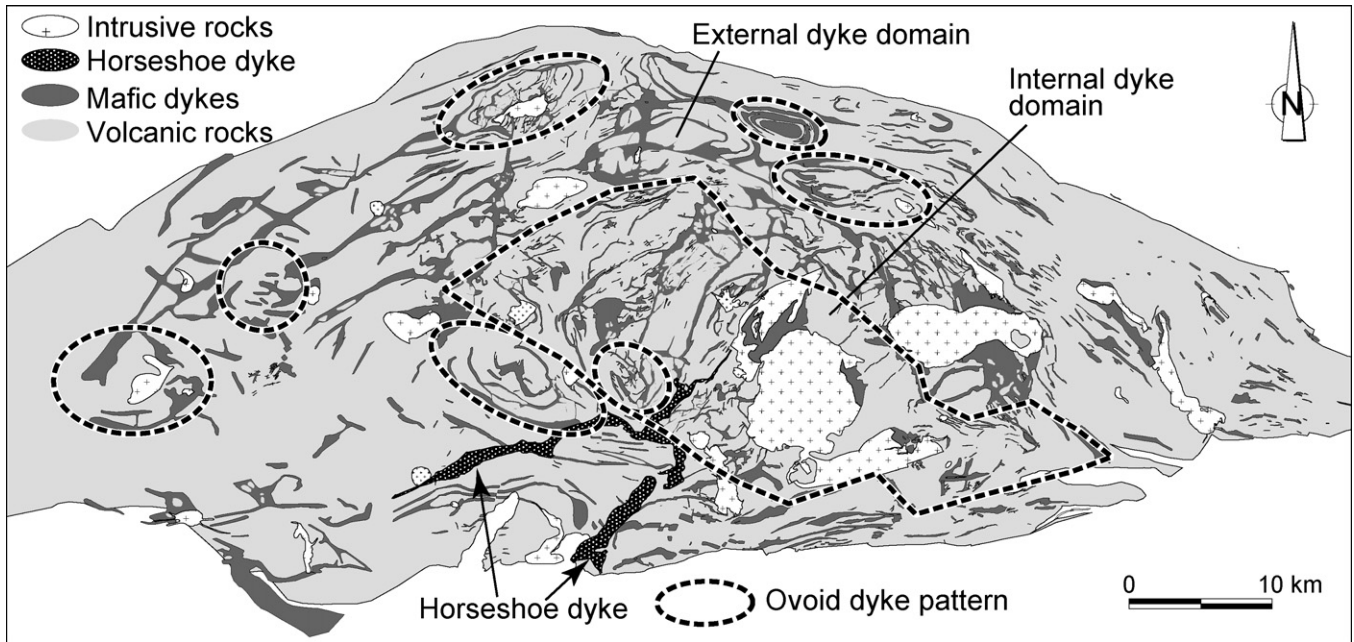


Fig. 3. Distribution of the mafic dyke swarms in the Blake River Group. Dashed lines highlight the main features discussed in the text. The external domain display ring and radial dykes punctuated by local ovoid dyke swarms. The internal domain is mostly characterized by crescent-shaped dykes around the Flavrian Pluton. The Horseshoe dyke is indicated in reference to the text.

dyke patterns are interpreted by Mueller et al. (2007) as outlining the volcanic centers, which are possibly the roots of summit calderas.

3.1.2. Internal and external dyke distribution

A density grid map of dykes shows a concentration at the periphery of the BRG (Fig. 4A). Without considering the ovoid dyke patterns, the BRG area can be subdivided into two main domains: (1) an internal and (2) an external dyke zone (Figs. 3 and 4). The internal dyke domain represents a NW-trending elongated zone, the boundaries of which are defined by abrupt changes in dyke directions. Dykes are generally thinner (median value = 172 m) and collectively trace an arc around the Flavrian Pluton, with NE and NW being the two dominant trends (Fig. 4C and E). The external dyke domain corresponds to a 10–20-km-thick envelope around the internal domain in which a concentric pattern is well established. Dykes measure 100–500-m thick (median = 212 m) with thicker and more continuous dykes by comparison with the internal domain (Fig. 4D and E). They collectively form an arc around the internal domain forming a radial pattern (Fig. 4B and D). The two dyke domains suggest two independent caldera-formation events.

3.1.3. Horseshoe dyke

A distinct triple junction dyke pattern stands out in the BRG, referred to here as the horseshoe dyke system. Locally exceeding 1-km thick and extending for more than 25 km, the Horseshoe dyke has two NE- and E-NE branches that curve toward each other and merge into one NE-trending segment. The dyke represents a composite intrusion of gabbros, diorites and quartz diorites. A peculiar phenomenon is observed around the southern branch where the volcanic assemblage displays south-facing younging directions on the west side, but north-facing directions on the east (Figs. 3 and 5). Hawaii rift zones with summit calderas display such a geometric

pattern and are characteristic of shield-building phases (Fiske and Jackson, 1972).

3.1.4. Interpretation of the dyke pattern

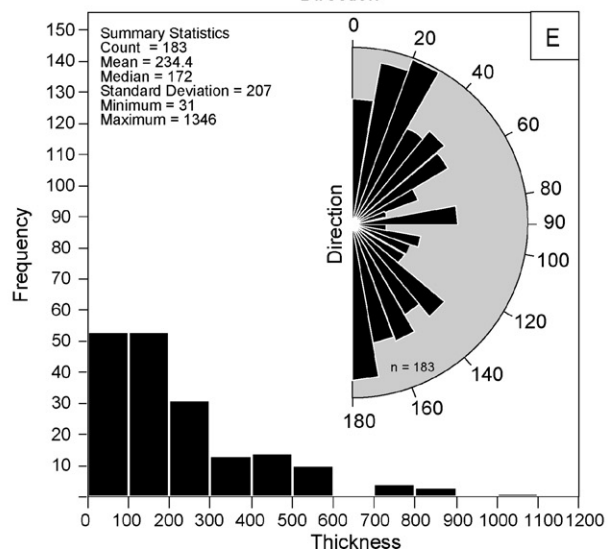
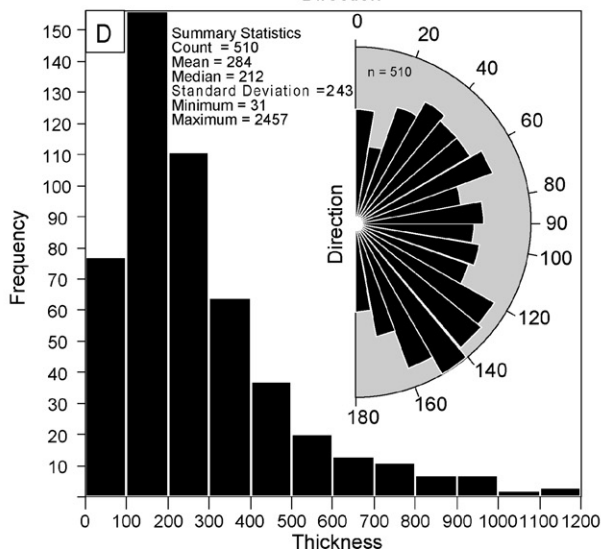
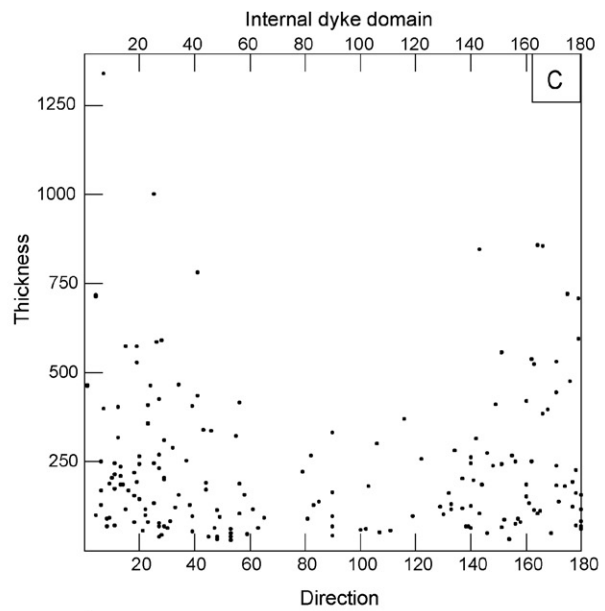
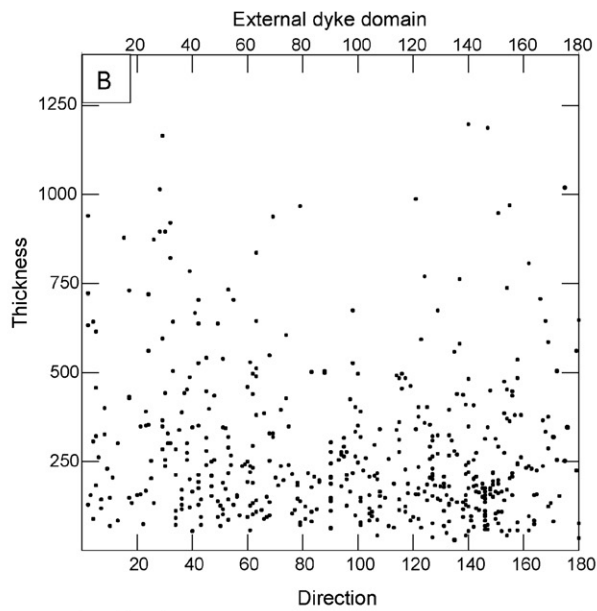
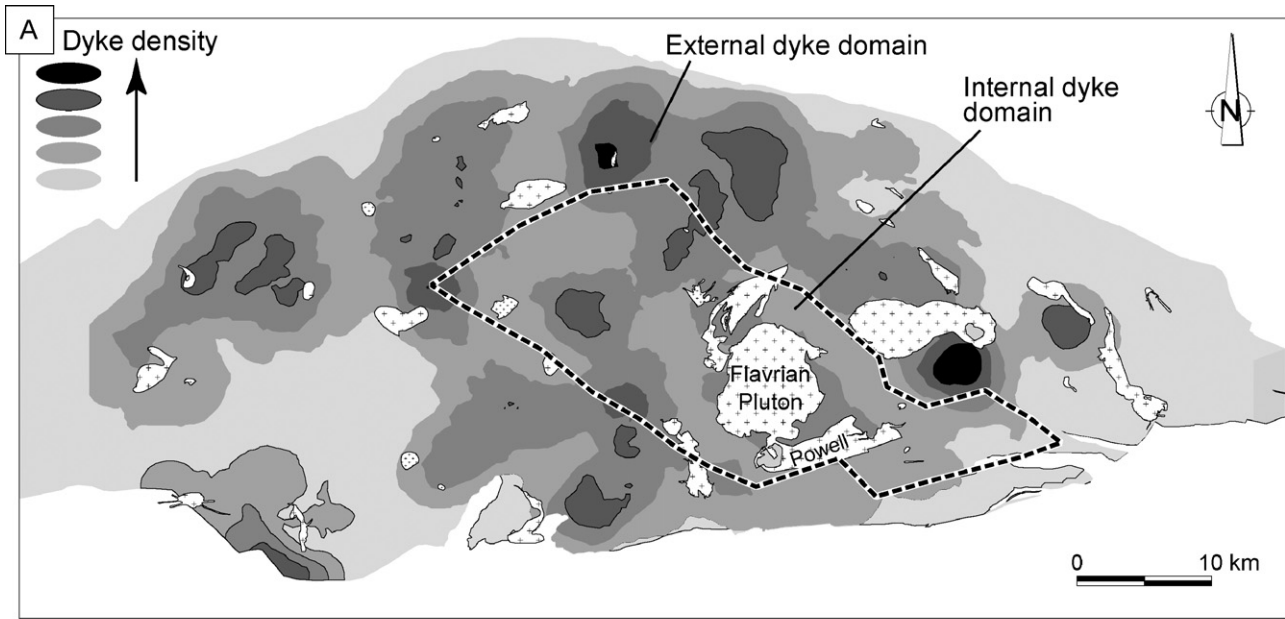
Most dykes are interpreted as endogenic growth intimately related to volcanic edifice construction, but others could be late- or post-volcanic. In such a scenario, dyke emplacement and configuration are likely to follow a fracture pattern (Anderson, 1937; Ernst et al., 1995), probably in response to a regional stress field and/or more local stress field related to the gravitational regime associated with the growth of a volcanic edifice. As long as the dykes have a subvertical dip, their surface traces provide a good estimation of the paleo-minimum compressive stress (σ_3) (Anderson, 1937; Gudmundsson, 2002). The deduced paleostress field highlights points of convergence that correspond to the Flavrian pluton and the local volcanic centers defined by ovoid dyke pattern. It is significant that two of these convergent points A and B in Fig. 5 represent the only areas where strata are subhorizontal (20–40°).

Some major dykes, e.g. the Horseshoe (south branch) and N-S dykes are not coherent with the stress field estimation (see Section 5), but the overall coherence and compatibility in the stress field trajectories deduced from the dyke patterns (coupled with age determinations) support the synvolcanic origin for the majority of the dykes.

3.2. Dome geometry

The integration of the bedding attitude into trajectories combined with younging directions enables a division of the BRG into two distinct areas (Fig. 6). The peripheral area defines an overall circular pattern characterized by steep strata with generally inward-younging directions, except for the western part. Local inversions of younging directions are observed mostly in the

Fig. 4. (A) Density grid map of dyke distribution for the Blake River Group showing an annular zone of higher dyke abundance within the External dyke domain, supporting the caldera interpretation. The binary diagrams in (B) and (C) compare dykes thickness and orientation. Distribution histogram and rose diagram in (D) and (E) display a similar relationship. They show thicker dykes occupying all directions in the external domain and two dominant dyke directions in the internal domain.



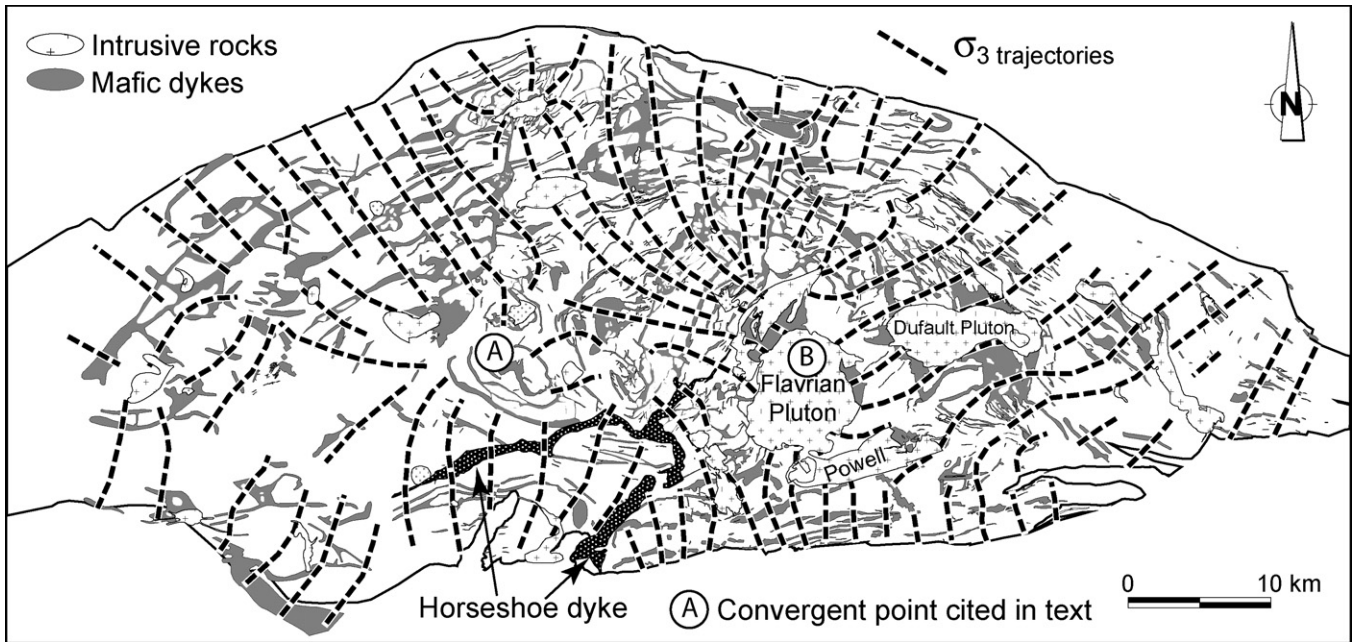


Fig. 5. Minimum stress trajectories deduced from dyke patterns in the Blake River Group. Note that the points of convergence correspond to the locations of the ovoid dyke swarms and to the Flavrian pluton. (A) and (B) convergent points are areas where strata dip gently (20–40°).

northern part of the peripheral area and are associated with discontinuous axial traces of doubly plunging folds. The central area defines a complex structural dome-shaped geometry with moderate to shallow-dipping units. The volcanic Duprat dome is the culmination of this central area. The flanks of the Duprat dome were steepened by late-stage shortening and can be interpreted as the locus of a regional antiformal axial trace that was already identified and interpreted by Goodwin (1965). The eastern side of the dome structure is homoclinal with gentle dip (30–45°) to the east (Gibson, 1989), and contains the Noranda Caldera. The Flavrian Pluton repre-

sents a window into the underlying high-level subvolcanic magma chamber (Goldie, 1979; Kennedy, 1984; Paradis et al., 1988). The western side of the volcanic Duprat dome structure is west-facing, homoclinal and extending to the Ben Nevis area (Pearson, 1994a, Figs. 2 and 6).

3.3. Faults

The BRG fault pattern (Fig. 7) is based on detailed field observations and data compilations combined with topographic and

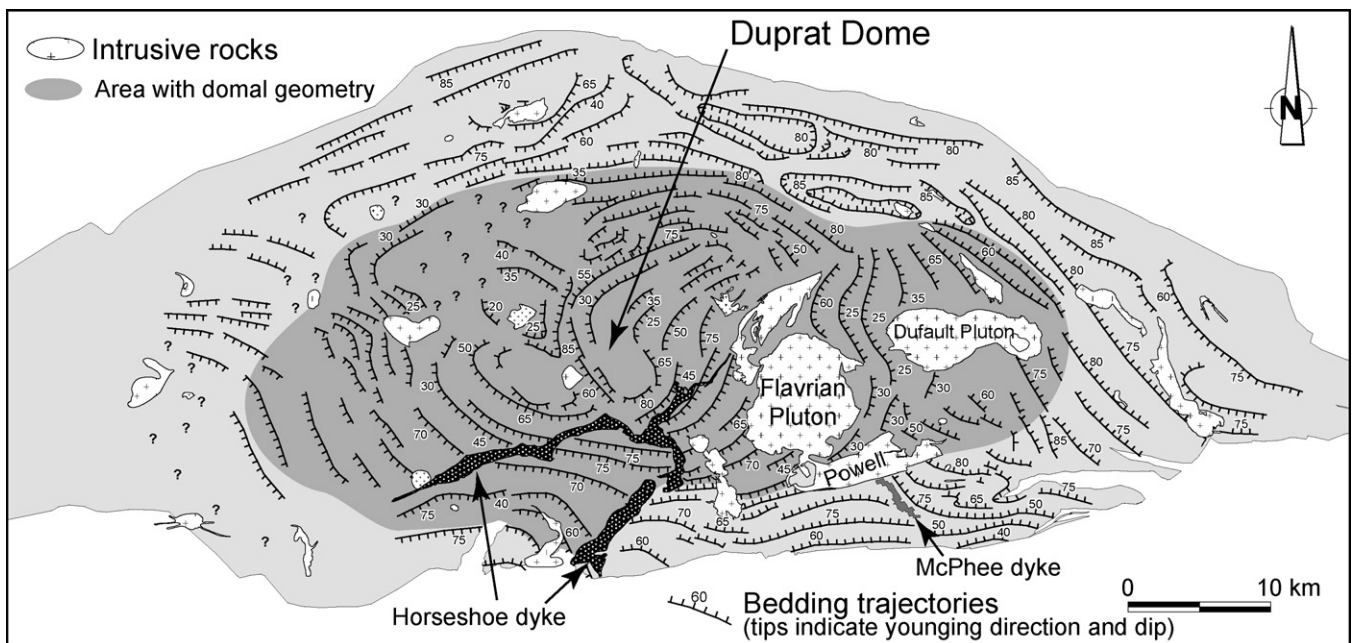


Fig. 6. Trajectories of bedding attitudes in the Blake River Group. The general architecture depicts an inner dome (Duprat) with gently to moderately outward-dipping strata. At the periphery, strata dip steeply, are typically inward-facing, and are locally affected by folding. Discontinuities in bedding trajectories are along synvolcanic faults and dykes, and along late faults.

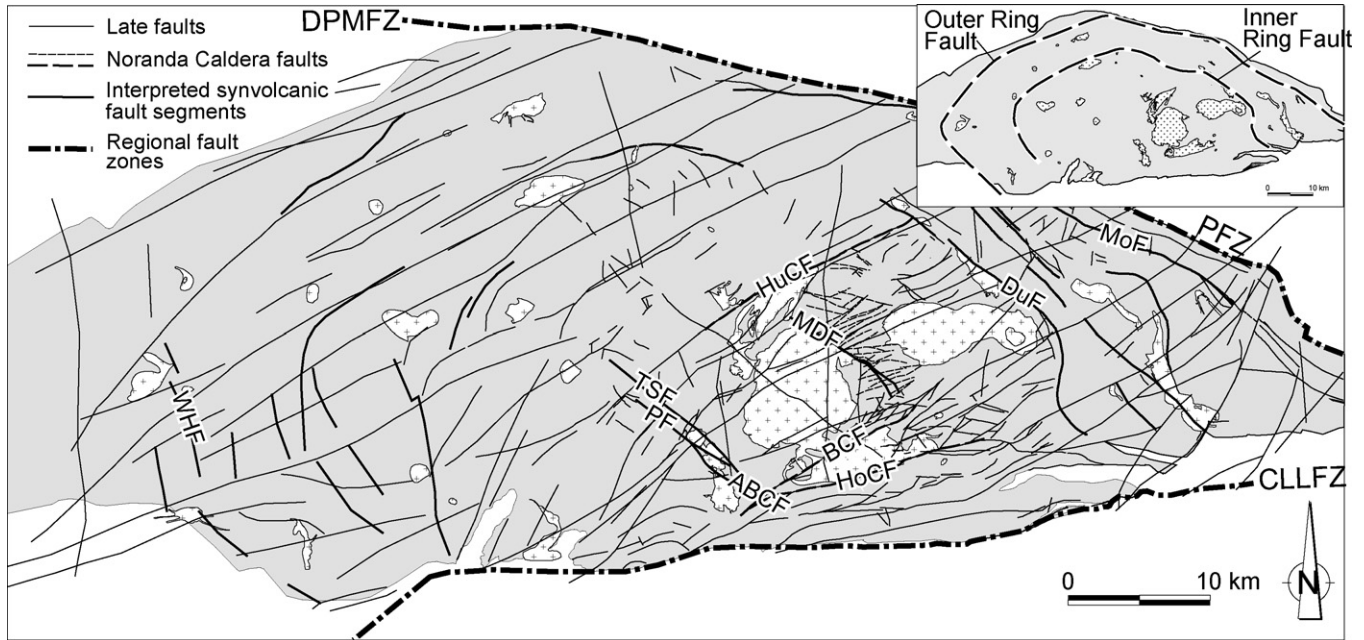


Fig. 7. Fault patterns in the Blake River Group (BRG) showing the dominant 070° -trending faults. The high fault density in the east-central part of the BRG is related to the Noranda Caldera. Thick lines represent earlier faults that are commonly curved, discontinuous and used, in combination with the dyke pattern, to define a double ring fault structure; see the inset map. HuCF: Hunter Creek Fault, BCF: Beauchastel Creek Fault, HoCF: Horne Creek Fault, DuF = Dufresnoy Fault, MoF = Mobrun Fault, WHF = Workman Hill Fault.

geophysical lineaments. Excluding the two well-known E-trending major fault zones (DPMFZ and CLLFZ) that limit the BRG, several fault sets were recognized on the basis of their orientation but most of them are generally interpreted to be late in the structural evolution (Daigneault and Archambault, 1990).

The 070° -trending faults set is more developed and affects the whole BRG with a mean spacing of 4 km. Although most faults have experienced a late component of movement as indicated by the presence of mylonites or cataclasites (indicative of brittle-ductile deformation), others such as the Hunter Creek, Beauchastel and Horne Creek faults are synvolcanic based on the control exerted

on the lithofacies distribution, the presence of hydrothermal alteration, and the intrusion of synvolcanic dykes (see Gibson et al., 1999).

Some fault segments, locally curvilinear and with dominant NNW and SE trends, are crosscut by late faults, especially by the 070° sets (Fig. 7). Among them is the NNW-trending Workman Hill fault (Hogg, 1964) and the SE-trending Mobrun and Dufrenoy fault which, in this latter case, lies along a synvolcanic intrusion (Goutier and Melançon, 2007). The extrapolation of early fault segments, combined with the traces of interpreted fractures as deduced from the dyke distribution, argues favourably for a BRG-wide annular

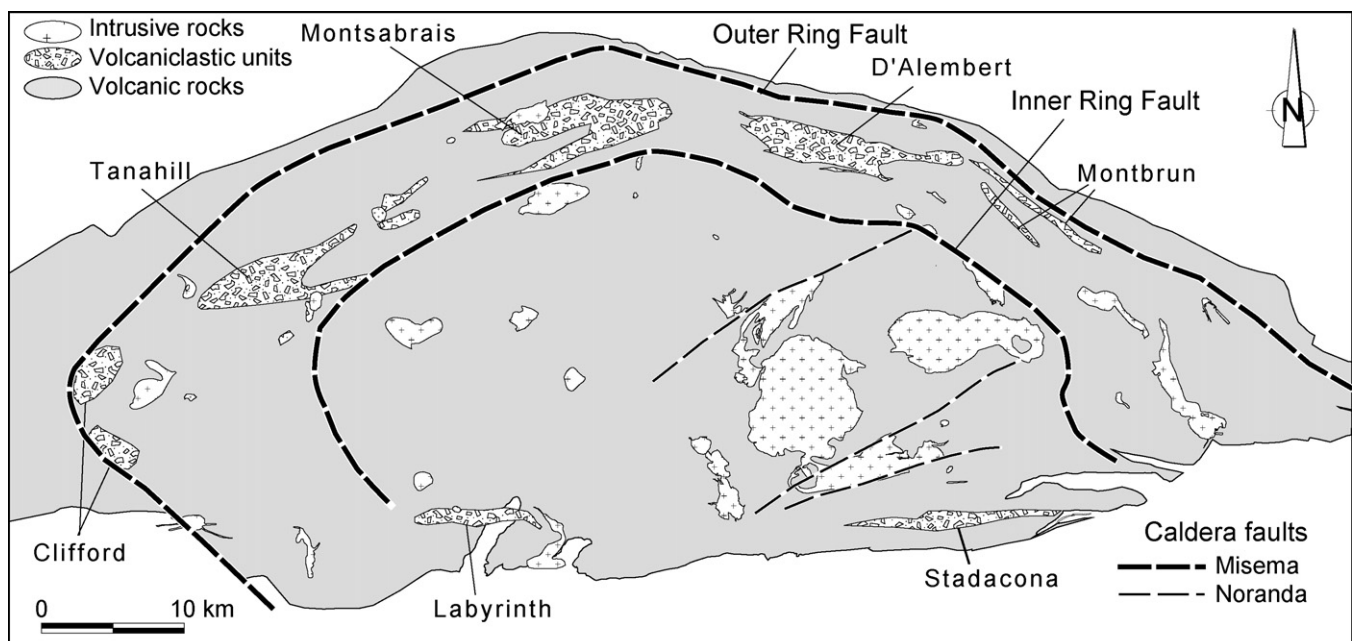


Fig. 8. Distribution of major volcanoclastic units in the Blake River Group with respect to the Inner and Outer Ring Faults of the Misema Caldera.

fault pattern. Two major annular faults are inferred. The Outer Ring Fault has a diameter of 65 km and is located at the periphery of the BRG. The Inner Ring Fault has a diameter of 45 km (Fig. 7) and is best documented by the SE-trending Dufresnoy Fault. Both ring faults are truncated by the CLLDZ in the south.

3.4. Distribution of volcanoclastic units

The Noranda Subgroup of the NC area is characterized by effusive volcanism with minor (less than 5%) pyroclastic deposits (de Rosen-Spence, 1976; Dimroth et al., 1982; Paradis et al., 1988; Gibson, 1989). On the other hand, abundant volcanoclastic units are distributed in a concentric fashion between the Inner- and Outer-ring faults of the BRG (Fig. 7). These major volcanoclastic units can be of pyroclastic (Tassé et al., 1978; Pilote et al., 2007) and possibly of autoclastic origin that may or may not be reworked to varying degrees.

The volcanoclastic units have an intermediate to mafic chemical composition and correspond to km-scale units, 1–3 km in thickness and traceable for 10–20 km along strike. Using the classification of Mueller and White (1992) for subaqueous pyroclastic deposits, they are variably represented by tuff, tuff breccias and lapill tuff breccias containing crystals, lithic, vitric, scoria and pumice and exhibiting massive or chaotic structure, graded and cross-bedded and channelled structures. The prominent volcanoclastic units of probable pyroclastic origin are those of Tannahill, Montsabrais, d'Alembert and Mobrùn which are located along the northern periphery of the BRG (Fig. 8). They have been inferred to erupt from submarine and possibly emerging vents (Jensen, 1978, 1981; Tassé et al., 1978; Dimroth and Desmarke, 1978; Dimroth and Rocheleau, 1979; Dimroth et al., 1982; Desgagné, 1995; Gagnon et al., 1995; Goutier, 1997), but all deposits are in a subaqueous setting, as indicated by bounding facies (Mueller et al., 2004).

The distribution of volcanoclastic units between the Inner and Outer Fault Rings (Fig. 8) may represent either a single chronological event or a multi-stage event, but the latter seems more probable

as these units occupied different stratigraphic levels. Furthermore distinct geochemical affinities from tholeiitic to transitional and calc-alkaline were recognized for several of these units (Ross et al., 2007).

This volcanism is strikingly different from the volcanism of the inner Noranda and New Senator part of the BRG. The presence of extensive mass flow deposits and their distribution between the Outer and the Inner Ring Faults require significant topographic relief and major collapse. The presence of a caldera wall associated with the Misema caldera event can accommodate all these attributes.

3.5. Carbonate-rich hydrothermal alteration

Archean hydrothermal conduits are identified by an alteration pattern, which include chloritization, sericitization, epidotization, and silicification at low metamorphic grades and is commonly associated with VMS mineralization. For the NC (Knuckey et al., 1982; Gibson, 1989; Cathles, 1993; Santaguida, 1999) this alteration pattern is constrained to the plumbing system and mimics the synvolcanic fault pattern. Hydrothermal carbonate alteration is associated with the Mattabi type deposits and occurs mostly as a large semi-conformable zone but may be present in more discrete disconformable zones (Morton and Franklin, 1987). Synvolcanic fractures are used as discharge zones for the hydrothermal fluids (e.g. Lafrance et al., 2000 and Lafrance, 2003), and display proximal Fe-rich carbonate varieties whereas Ca-rich carbonate varieties are prominent at distal locations (Mueller et al., 2008). Mueller et al. (2008) have shown that such hydrothermal patterns are inherent to Archean subaqueous calderas.

Fig. 9 displays the distribution of carbonate alteration defined from field observations combined with numerous geochemical analyses in the BRG (unpublished databases CONSOREM and related companies). Numerous zones of pervasive carbonate-rich hydrothermal alteration (ankerite and locally siderite) are not related to late deformation zones and quartz veining (Fig. 9). The

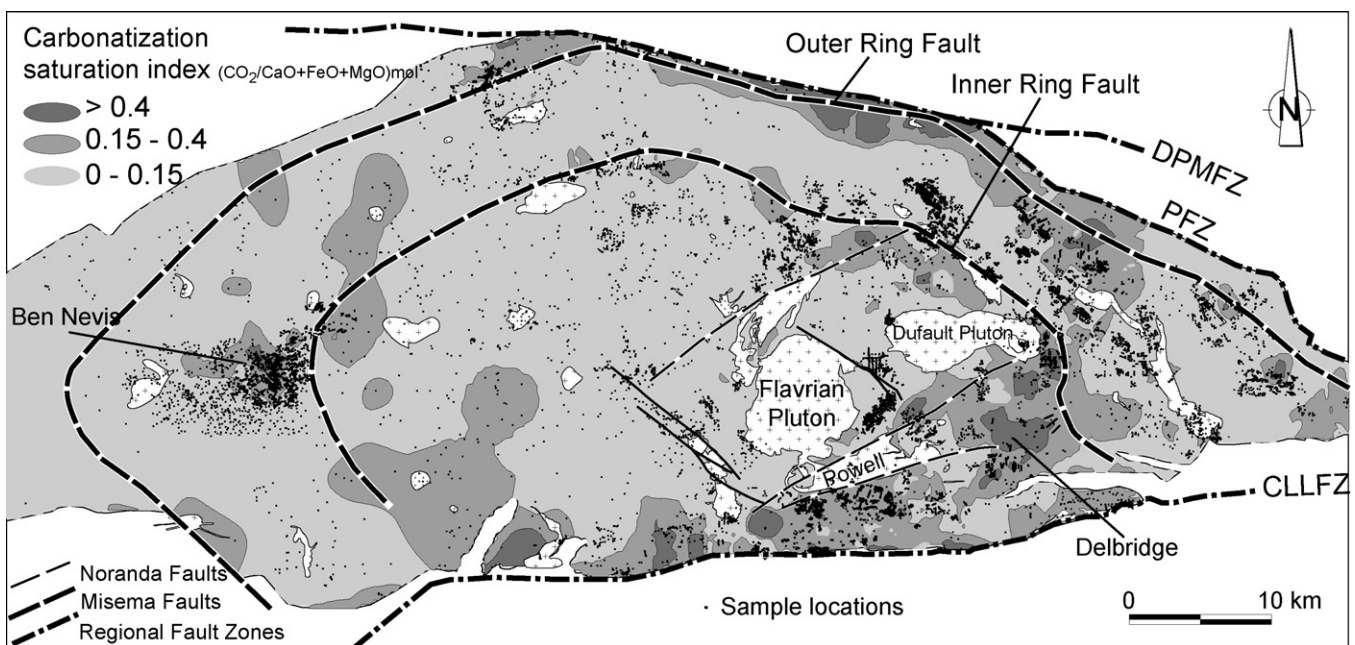


Fig. 9. Carbonatization pattern in the Blake River Group as established by the carbonate saturation index $\text{CO}_2/(\text{CaO} + \text{FeO} + \text{MgO})_{\text{mol}}$ (Nabil, 2007) calculated from litho-geochemical analysis from rock sample (CONSOREM's companies databases). The index determines the level of carbonatization independently of rock composition. Calculated index values were combined with the modal carbonatization observed in the field, revealing that the inner part of the BRG is virtually unaffected by carbonatization although strong and pervasive areas of ankerite + calcite (\pm siderite) occur along the Inner and Outer Ring Faults of the Misema Caldera. A carbonate-rich envelope is also found along the Destor-Porcupine-Manneville Fault Zone (DPMFZ) and the Cadillac-Larder Lake Fault Zone (CLLFZ).

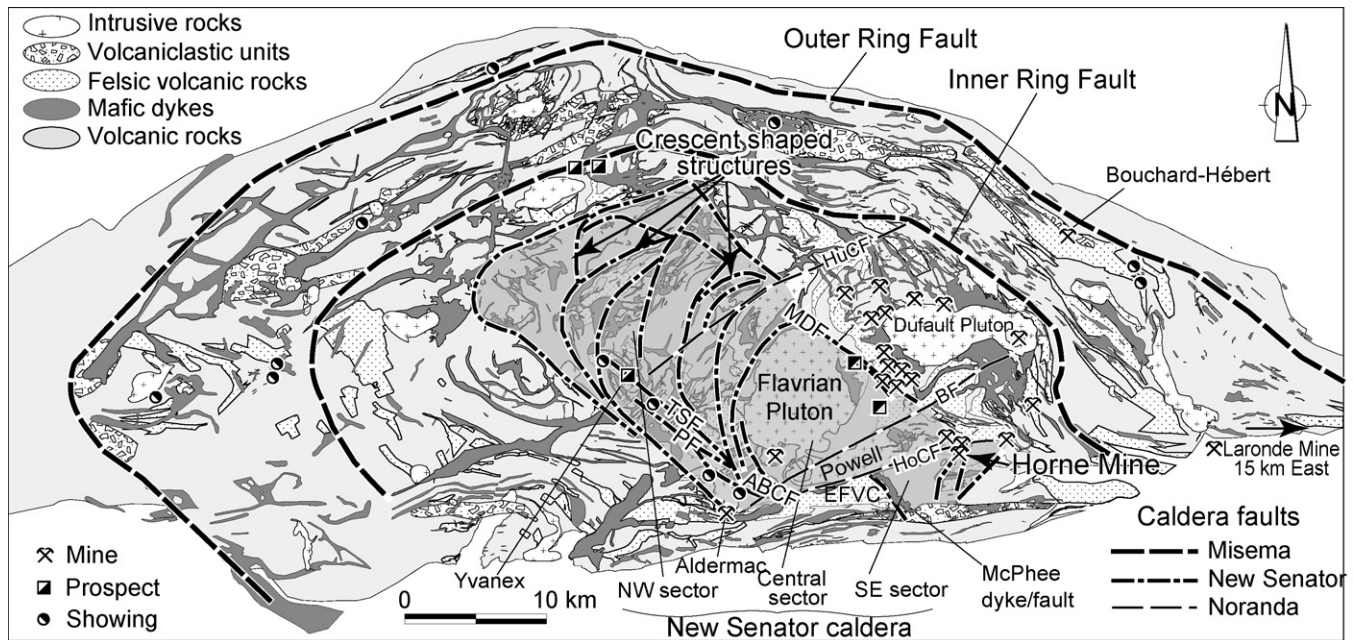


Fig. 10. Misema Caldera major fault system and delineation of the New Senator Caldera. The distribution of VMS mineralization is shown with respect to synvolcanic structures. Deposits in the Noranda camp are intimately associated with the Noranda Caldera faults. The Yvanex-Aldermac group is closely related to the western limit of the New Senator Caldera faults. Finally, peripheral mineralizations are associated with the Misema Caldera fault system.

Ben Nevis area displays a zone of intense carbonatization related to VMS alteration (Grunsky, 1986; Pearson, 1994a; Hannington et al., 2003, Fig. 9) and the large pervasive carbonatized zone in the Delbridge area (Fig. 9) is not associated with any ductile deformation (Barrett et al., 1992). Carbonatization is also common to gold deposits, and could be produced by orogenic gold-bearing vein systems associated with the DPMFZ, CCLFZ and related fault splays (Daigneault et al., 2002). However in this case, the carbonate distribution in the BRG follows a pattern constrained by the Outer and Inner Ring Faults. This distinct pattern is not associated with late shear zones but rather with synvolcanic faults.

4. The New Senator Caldera

The New Senator Caldera (NSC) requires special attention for its particular link to VMS mineralization in the BRG. The NSC is a 35 by 14 km elongated NW-trending structure lying in the center of the BRG (Fig. 10). It is defined by two major bounding NW-trending fault zones that delineate the internal dyke swarm. The NSC is overprinted by the Noranda Caldera event since fractures associated with the NSC are crosscut by 070°-trending Noranda Caldera fractures. The NSC is described below according to three sectors (Fig. 10).

(1) The sector south of the Horne Creek Fault (Fig. 10) displays a north-facing homoclinal sequence and presents two different families of synvolcanic fractures. The 340° McPhee fault (Fig. 10) is synvolcanic based on the presence of the intruding McPhee gabbroic dyke that separates two different volcanic sequences and a significant volcanic facies change. To the west of the fault, the Evain felsic volcanic complex (EFVC) is composed of coalesced subaqueous rhyolitic domes. To the east of the fault, a mafic-dominated complex interpreted as a lava lake or high effusion flows is present (Pearson, 1994b). Voluminous cogenetic dykes cut the sequence.

East of the McPhee fault, the strata change from NW-trending proximal to the fault to E-trending farther away (Figs. 6 and 10). After rotation of the subvertical strata to their original sub-horizontal position, this change in bedding attitude can be interpreted as a drag fold associated with a synvolcanic normal fault, and supports the collapse associated with the NSC. The McPhee fault is crosscut by the 070°-trending Horne Creek Fault of the Noranda Caldera, which infers that sector collapse along the McPhee fault and mafic lava lake formation predate Noranda Caldera formation.

- (2) The central sector between the Hunter Creek Fault and Horne Creek Fault of the Noranda Caldera is occupied by the Flavrian and Powell plutons (Fig. 10). The southwestern boundary corresponds to a series of NW-trending synvolcanic faults (Fig. 10), including the “ABC” fault (Pearson, 1986), the TS and Pink faults (Falconbridge Copper, unpubl. Open file assessment reports), as well as the intrusions occupying the synvolcanic faults (Dion and Legault, 2005). The northeastern part is partly obscured by the 070° fractures associated with the Noranda Caldera, but the 320°-trending McDougall–Despina fault (e.g. Setterfield, 1987) is considered the northeastern limit of the NSC. This fault displays a dip-slip collapse of more than 750 m for the southwestern block (Setterfield et al., 1995) and is crosscut by the 070° faults of the NC.
- (3) The sector north of the Hunter Creek Fault is dominated by volcanic rocks. Several felsic domes such as Inmont and Duprat (Fig. 2) are recognized. Discrete chert horizons are found around felsic domes. The distribution of mafic dykes and felsic volcanic centers, combined with lineaments interpreted from aeromagnetic surveys, led to the definition of arc- or crescent-shaped areas that mimic the shape of the Flavrian Pluton.

5. Discussion

The volcanic architecture of the BRG has been interpreted as a volcanic complex (Goodwin and Ridler, 1970; Goodwin, 1977, 1979, 1982). The proposed litho- and chemo-stratigraphic subdivi-

sions were explained as a large synclinorium with a central dome in which structural elements reflect the combined influence of volcanic construction, subjacent intrusions and late tectonic deformation (Goodwin, 1965; Jensen, 1981; Dimroth et al., 1982). Based on this study previous geological observations are re-interpreted below following new concepts of modern subaqueous volcanic edifices and calderas, as well as rheological models.

5.1. Dyke and fault patterns

Recent advances in the structural analysis of volcanic edifices have highlighted the importance of dykes, of which only a small proportion ever reach the surface (Gudmundsson et al., 1999; Takada, 1999; Gudmundsson, 2002). Typically, endogenous growth accounts for a significant part of the long-term history of an edifice (Annen et al., 2001) and helps modify internal stresses (Walter and Troll, 2003; McGuire and Pullen, 1989). The primary control on a dyke's orientation follows Andersonian faulting rules (Anderson, 1937), where the initial setting of the stress ellipsoid is provided by the regional tectonic regime (Nakamura, 1977; Ernst et al., 1995; Walker, 1999). Importantly, with the growth of the edifice, the gravitational stress regime can supersede the regional regime and modify the structural evolution path (McGuire and Pullen, 1989). For example, the Iceland volcanic field is characterized by two dyke systems: a regional vertical dyke system and a ring sheet dyke system, both of which reflect the regional and proximal subvolcanic stress field (Gudmundsson, 2002). In Tenerife (Marinoni and Gudmundsson, 2000), the preferential orientation of dykes was used to define a regional minimum stress. In the Taupo volcanic field, the multi-caldera setting is emphasized by a regional subparallel fault system associated with the tectonic regime (Kissling and Weir, 2005).

In the BRG, the ring geometry exhibited by the mafic dyke and fault systems is strikingly different from systems elsewhere that are related to the horizontal field stress characteristic of convergent or divergent plate settings (see Ernst et al., 1995). Experimental (Gray and Monaghan, 2004), analog (Acocella et al., 2000; Roche et al., 2000; Walter and Troll, 2001), and natural examples (Cole et al., 2005) of ring structures suggest a withdrawal of material leading to surface depressions, such as down-sagging and caldera formation. Extension is expressed by ring fractures.

The geometry of the Horseshoe gabbro/diorite dyke (Fig. 2) shares numerous geometric features of radial structures that define a paleo-stress field in which magmatic pressure surpasses lithostatic pressure (Smith, 1987; Ryan, 1988). This geometry, called "rift" structure, is well documented for the oceanic volcanic islands of Hawaii (Dieterich, 1988) and Tenerife (Carracedo, 1994), as well as from analog models (Walter and Troll, 2003). These structures are considered by Walker (1999) as intrinsic evolutionary features of oceanic island volcanoes and are ubiquitous for volcanic edifices taller than 3 km (Walter and Troll, 2003). The expression of the stress distribution in rifts are linear, en echelon, or curved. The presence of a ternary point in the Horseshoe rift is indicative of specific conditions where internal stresses exceed regional stresses (McGuire and Pullen, 1989; Walter and Troll, 2003). Furthermore, an inversion of younging directions across the rift arms supports the idea of a long-lived accommodation structure and sector collapse (e.g. Carracedo, 1994; Tibaldi, 2003). Such structures represent the fundamental elements of a volcanic complex underlain by its magmatic source. They experience and register multiple magmatic pulses as indicated by the variety of rock types. Periods of magmatic inflation promote the creation of complex "Horseshoe"-type rift zones and sector collapses. Periods of magmatic retreats permit down-sagging with extensional ring fractures that are eventually invaded by subsequent magmatic pulses. Similarly, the N-trending

dykes that crosscut the general ring dyke pattern, are an expression of such magmato-tectonic events.

Stratigraphic evidence was used to demonstrate the collapse along Noranda caldera (Gibson, 1989). Similar arguments were used for the McDougall–Despina fault (Setterfield, 1987), which represents the eastern limit of the New Senator Caldera. These stratigraphic analyses were performed in an area characterized by low-dipping strata (20–30°). For the Misema caldera no such stratigraphic evidence can be used because of the near vertical position of both the Outer Ring Fault and the volcanic units (Fig. 6). However, the presence of the abundant volcanic debris between the Outer and Inner Ring Faults strongly support a major collapse event for the Misema caldera, as significant topographic relief is required (Mueller and Mortensen, 2002).

In addition, the peculiar geometry of the New Senator Caldera crescent-shaped faults requires attention (Fig. 10). These structures define the physical limits of the ovoid dyke complexes (rare dykes crosscut the structures) and they circumscribe the felsic extrusive complexes. The fault geometry suggests that the New Senator Caldera was the result of sequential collapses, partly coeval with the construction of volcanic centers and collectively accounting for the complex architecture. The New Senator Caldera displays the characteristics of an overlapping collapse caldera and is best explained by southeastward migration of an underlying magmatic chamber. As has been proposed for the Las Cañadas caldera in Tenerife (Marti and Gudmundsson, 2000), each collapse step imposes a change to the local field stress and promotes the rejuvenation of the magmatic chamber along one side of the chamber. The various collapse steps culminated with the formation of the Noranda Caldera in the southeast. In this segment the Flavrian–Powell intrusive complex developed. The eastward migration of volcanic activity and related collapses are in good accordance with previous interpretations (Goodwin, 1965, 1977, 1979; de Rosen–Spence, 1976; Dimroth et al., 1982).

5.2. A giant magma chamber

The caldera model has implications for the architecture of the BRG. Recent developments in the understanding of caldera collapse (Roche et al., 2000; Walter and Troll, 2001, 2003; Acocella, 2007) show that outer and inner ring faults are ubiquitous features in rheologic models. The inner ring faults of the Misema caldera (Figs. 7 and 10) are interpreted to represent a reverse extensional and outward-dipping fault. All experimental models show that gravitational instability in the overlying wedge triggers collapse with the development of an outer ring fault, which is likely to be normal and inward-dipping.

An important point recently highlighted in rheologic models is the relationship between the diameter of the outer ring fault and the underlying magma chamber. This relationship implies that a plutonic mass having approximately the diameter of the outer ring fault must exist under the BRG (i.e. Gudmundsson, 1998a,b; Walter and Troll, 2001; Gudmundsson et al., 1997). Although the presence of such a plutonic mass is speculative, indirect support is provided by the presence of subhorizontal reflectors detected in seismic profiles (LITHOPROBE) at around 1.5–3 s travel time, which have been interpreted as intra-plate tonalites (Jackson et al., 1990; Green et al., 1990; Clowes et al., 1992; Ludden et al., 1993). The approximate dimensions of this intrusive mass (informally called the *Misema Pluton*) would be around 40 km × 75 km, representing an aerial extent of 3000 km². This is not exceptional in the geological record. By comparison, caldera-forming events of Yellowstone produced more than 4800 km³ of ash flows over a period of 2 Ma (Christiansen, 1984, 1994) and a giant magma chamber probably of the same order to the BRMCC.

In Taupo, the study of seismic velocity and CO₂ saturation in melt inclusions suggest a 2–4 km-thick zone of partial melting at a depth of 4–8 km under the 10 km × 20 km Oruanui caldera (Wilson et al., 2006). This proposal has implications for the 3D architecture of the BRG as it implies at least two levels of magma generation/accumulation (e.g. Misema Pluton and the high level Flavrian-Powell system). The reservoirs were fed from a deeper source and define a three-step architecture similar to the Taupo rift zone (Charlier et al., 2005; Wilson et al., 2006) and the San Juan volcanic field (Bachmann et al., 2002). Despite the different tectonic settings of Taupo and BRMCC, the crustal architecture and distribution of melt products can be compared. This multi-level setting explains in an efficient manner the distinct geochemical signatures. The Misema Subgroup was generated from a primary deep magmatic source (Baragar, 1968; Goodwin, 1982), whereas the Noranda Subgroup is interpreted as a product of high-level magma chambers (Gélinas and Ludden, 1984; Ujike and Goodwin, 1987; Hart et al., 2004).

5.3. Late intrusions

The volcanic history of the BRG terminated with the final emplacement of plutons and stocks, the largest being the Dufault Pluton (2696 Ma). Most of these intrusions do not have extrusive counterparts recognized in the stratigraphic record. The location of synvolcanic and late intrusions is in close relationship with the volcanic architecture and pre-existing structure. The emplacement of these plutons is interpreted to be influenced by synvolcanic anisotropies, such as volcanic centers and faults. Collectively, intrusions concentrate along the fractures related to the Misema, New Senator and Noranda Calderas.

5.4. Evolutionary model for the megacaldera complex

5.4.1. Stage 1—multi-vent shield volcano

The development history of the BRG (Fig. 11) began with the progressive build-up of a multi-vent mafic shield volcanic complex (i.e. Baragar, 1968; Goodwin, 1979; Jensen, 1981; Dimroth et al., 1982; Fowler and Jensen, 1989) as the result of deep-source magmatism (garnet-in stability field), represented by the Misema Subgroup. This superstructure formed above the submarine tholeiitic basalt plain of the Garrison Subgroup (Goodwin, 1977; equivalent to Kinojevis of Jensen, 1981 and Lower Blake River of Ayer et al., 2005).

Progressive growth of the edifice modified the internal stress field, and relaxation is partially accommodated via down-warping and rift development. The Horseshoe structure represents an important component of the rift system. Inversion of younging directions from side to side along the Horseshoe dyke supports its interpretation as a collapse sector in the edifice. Magmatic activity and subsidence of the incipient megavolcano caused a thermal rise that triggered the partial melting of the crust and was subsequently responsible for the genesis and growth of an underlying plutonic mass at an approximate depth of 3–5 km (Fig. 11a).

5.4.2. Stage 2—first collapse event: the Misema caldera

The second stage features the underlying magma chamber developing coevally with growth of the volcanic edifice and associated dyke swarm. The first caldera collapse event represented by the Misema Caldera, was characterized by the formation of Outer and Inner Ring Faults and the emplacement of major subaqueous pyroclastic and autoclastic debris (Fig. 11B). This catastrophic event(s) had a profound influence on the evolution of the BRG, as it represents a change from effusive- to explosive-dominated volcanism and a chronostratigraphic shift from the mafic Misema Subgroup to the bimodal mafic-felsic Noranda Subgroup. The exact

nature of the collapse remains a subject for further work and a multi-step process in space and time can be envisaged. Furthermore, the collapse need not have been homogeneous, and could have varied from discrete faults to local warping.

The caldera collapse efficiently promoted a net of interconnected faults that increased secondary structural porosity and enhanced hydrothermal activity. The restricted distribution of carbonate alteration along the ring fault system strongly supports a hydrothermal CO₂-rich period. Carbonatization in the inner part of the caldera cannot be ruled out, but if present, was probably obscured by the Noranda Caldera volcanism.

5.4.3. Stage 3—central resurgence

Renewed volcanism of the Noranda Subgroup was derived from a garnet/amphibole-free source, although local effusion from a deep depleted source, including magma mixing and contamination (Lafliche et al., 1992; Pêloquin, 2000), occurred. This volcanism produced a bimodal multi-vent volcanic structure with major felsic effusion centers. A source for the Noranda Subgroup is the unexposed, postulated Misema Pluton. A resurgent central dome (20 km × 30 km with a NW long axis) inside the Misema caldera (Fig. 11c) developed, and obscured evidence of pyroclastic deposition and moat sedimentation. The Fishroe-type rhyolites with a chemically distinct composition are an important effusive event in the history of the resurgent dome (Ludden and Pêloquin, 1996), as they intrude the dome periphery. A high level magma chamber developed coevally, and this chamber is considered the incipient stage of Flavrian-Powell intrusive complex, because a sustained history of volcanic activity is inherent to volcanic edifices (Goldie, 1979; Paradis et al., 1988). Based on the spilitization and epidotization affecting such intrusions (Kennedy, 1984; Galley and van Breemen, 2002), it is reasonable to assume hydrothermal fields around the dome.

5.4.4. Stage 4—second collapse event, the New Senator Caldera (NSC)

The NSC represents a multi-step collapse stage. As suggested by the synvolcanic fault geometry, the first collapse event occurred along the northwestern limit of the NSC (Fig. 11D). Crescent-shaped structures developed sequentially from NW to SE, with a parallel migration of effusion centers. Effusion and collapse events were interspersed by short periods of quiescence as indicated by discrete chert horizons around the felsic domes. Caldera development is controlled by a southeastward migration of the underlying pluton. Most of the NSC events point to an incremental collapse punctuated by flows and domes. The closing event of the multi-step NSC stage occurred at the SE margin where the felsic pyroclastic activity, the inferred Horne pyroclastics, followed the development of voluminous lava lakes. The eastward migration of the thermal source is in good agreement with the conclusions of earlier studies (Goodwin, 1977, 1982; Capdevilla et al., 1982; Pêloquin, 1999).

The synvolcanic structure of the NSC is among the most important fracture systems associated with hydrothermal activity. Alteration and mineralization occurred along the SW and NE limits of the caldera and appear to have increased in abundance and intensity from NW to SE. This pattern mimics the migration of the underlying pluton and likely reflects the intensity and longevity of the thermal source which stabilized toward the SE. The Horne deposit located at the SE corner of the NSC is interpreted to be associated with fractures related to the NSC formation.

5.4.5. Stage 5—third collapse event, the Noranda caldera

A third collapse event forming the Noranda Caldera, occurred where high level magmatic chambers had stabilized, e.g. the Flavrian-Powell Plutons. This caldera overlaps the NSC and extends

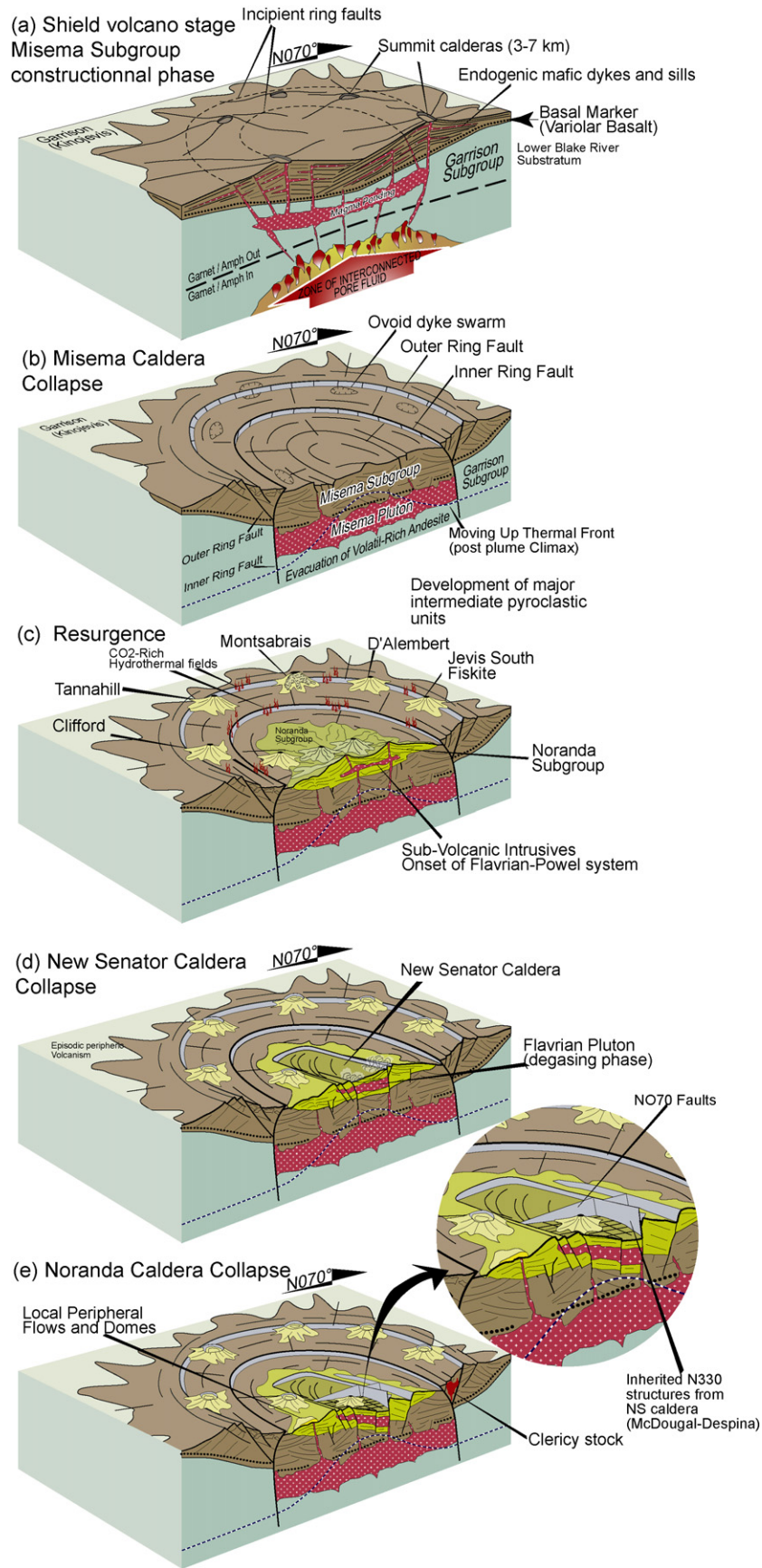


Fig. 11. Schematic diagrams illustrating the proposed evolution of the Blake River Megacaldera Complex.

eastward along ENE-trending Hunter Creek, Beauchastel Creek and Horne Creek faults (Gibson, 1989; Fig. 11e). The Noranda Caldera is interpreted as an incremental collapse event, as suggested by the distribution of infilling volcanic rocks and the absence of associated pyroclastic deposits (de Rosen-Spence, 1976; Gibson, 1989). The collapse generated a well-developed fracture pattern with a mean 070° trend, locally intruded by mafic and felsic dykes (Waite dyke complex, Gibson, 1989) that formed the central Noranda camp. Quiescent periods are indicated by the C and Main contact chert horizons. Some pre-existing structures related to the NSC were re-activated and are now recognized by their crosscutting relationships (e.g. McDougall–Despina faults). Along this fracture system VMS deposits continued to develop.

5.4.6. Concurrent events—stages 1–5

Coeval with the development of this megavolcanic structure is the emplacement of dykes. They inflated the edifice at least 15% and possibly as much as 30% by volume, based on calculations of the actual surface occupied by dykes with respect to the overall Blake River surface. The distribution of the mafic dykes (Fig. 3) suggests a homogeneous system characterized by fine- to coarse-grained hornblende gabbros, diorites and quartz diorites. The dykes were emplaced over a protracted period, encompassing all the volcanic activity.

At each caldera stage, renewed volcanism commenced along zones of initial weakness, including the peripheral margin of the Misema caldera. This precludes any simple relationship between collapse and magmatic events. Magmatism exploits any zone of weakness, irrespective of place, and therefore diachronous dome ages would be common (e.g. Valles Caldera, Goff et al., 1989; Self et al., 1996).

5.5. Impact on volcanic stratigraphy

The interpretation of the BRG as a megacaldera complex provides not only a sensible explanation for the faults, dykes and subaqueous pyroclastic rocks, but also effectively explains the distribution of lithological units in the Misema and the Noranda subgroups. The latter represents a resurgent bimodal dome over which New Senator and Noranda calderas developed.

The proposed model suggests that the BRG stratigraphy must be addressed from a volcanological standpoint by considering individual effusion centers over *time and space* and distributed over a minimum area of 2500 km². Therefore volcanic activity occurred in different locations contemporaneously, as indicated by coeval volcanism in the Ben Nevis, Montbrun and Millenbach areas. Late structural complexities are not required to explain volcanic center distributions.

The major change in the volcanic style from effusive flows and domes, to volcanoclastic-pyroclastic deposits is indicative of a major collapse event along the Outer Ring Fault with multiple events that defined ultimately the Misema Caldera. These deposits are thick accumulations near caldera margin faults, but elsewhere were eroded or covered by subsequent caldera-forming phases.

5.6. Effect of deformation

The volcanic architecture of the BRG represents a highly anisotropic medium, expressed by local volcanic centers with different rock types, collapse features with various orientations, and intrusive masses with different shapes and volumes. The proposed concealed Misema Pluton provides a good explanation for the relative low-strain domain that characterizes the BRG. This can be viewed as the result of stress distribution around the pluton, which acted as a buttress preserving the overlying volcanic rocks. This

process was already invoked for the Noranda dome (Dimroth et al., 1983; Goutier, 1997). Deformation was concentrated in the periphery of the BRG where lithological units, sills, and sheet dykes are folded and foliated. Conversely, subvertical features like feeder dykes and caldera faults can only be flattened, reactivated and overprinted by ductile deformation. The primary geometrical relationships are preserved, even after deformation. This last point is important because it enables the volcanic interpretation to be resolved despite the occurrence of a shortening component related to regional deformation.

Previously recognized axial traces of folds along the NE limit of the BRG are considered to partially express primary anisotropies in the architecture of the volcanic rocks. Paleogeographic reconstructions for this area (Tassé et al., 1978; Jensen, 1981; Dimroth et al., 1982, 1983; Fowler and Jensen, 1989) identified individual volcanic centers, including Montsabrais, D'Alembert, Montbrun, Clifford, Clarice, Tannahill, and McDiarmid Lake. They represent peripheral volcanic centers distributed along the Misema Caldera ring faults.

Even though local ductile deformation can be identified, the proposed model can explain the characteristics of the BRG on a regional scale. The local structural response can be used to reveal and emphasize primary volcanic features. Primary anisotropies act as loci for deformation nucleation. For example, subvertical dips may in part be caused by shortening of previously tilted panels along synvolcanic faults, ductile fabrics (e.g. schistosity and stretching lineations) may be enhanced by volcanogenic hydrothermal alteration zones, and local antiforms may reflect volcanic domes. Domal structures explain the discontinuous fold axial traces and local doubly plunging structural anticlines or synclines. However, local fold axial traces could also be the result of the shortening component affecting originally N-trending strata.

Synvolcanic faults were re-activated, and depending on their orientation and dip relative to the principal compressive stress, they developed “shear” characteristics, or were dismembered and obscured. Volcanic complexes, with their broad dome architecture, were flattened with steepened flanks and produced local plunging folds. Planar elements in the edifices, such as synvolcanic dykes and faults that share a subvertical primary attitude, were only translated keeping the original geometry.

5.7. VMS distribution and alteration pattern

The current interpretation of VMS distribution in the BRG is based on the historical Noranda camp with its 13 deposits (Gibson and Watkinson, 1990). Convincing arguments based on 3D-GIS models (Martin and Masson, 2005; Masson, 2005) have clearly emphasized relationships between synvolcanic faults, hydrothermal alteration, stringer zones, specific chert horizons and deposit locations. A linear distribution for massive sulphide lenses was recognized at the deposit scale (Knuckey et al., 1982), but also at the mining camp scale. Scott (1980) proposed a 330 lineament from Horne to Ansil; another 330 lineament was informally proposed from Aldermac to New-Insco. Although of great interest, it was difficult to take the next step in terms of predictive exploration strategies, particularly with respect to other unexplained VMS deposits. The overlapping or nested caldera model provides an effective way to explain the other VMS deposits. Three groups of deposits, including showings, prospects and mines, with distinctive characteristics are proposed.

The first group, recognized as the historical Noranda camp hosting 13 mines (Gibson and Watkinson, 1990), is associated with the 070° synvolcanic faults of the Noranda Caldera (Figs. 2 and 10). The nested caldera model allows an additional link. The Noranda Caldera most certainly inherited structures from the New Sena-

tor Caldera, especially the McDougall–Despina faults. These two are interpreted as reactivated older structures associated with the paleo-hydrothermal field of the New Senator Caldera.

The second group of deposits along the southwestern limit of the New Senator Caldera and associated with local volcanic centers in this area, includes old and recent VMS discoveries (Martin and Masson, 2005). Because the giant Horne deposit is associated with a N-trending synvolcanic structure (Kerr and Mason, 1990; Price, 1948), it is considered to be related to the New Senator Caldera rather than the Noranda Caldera.

The third group is linked to the BRG peripheral ring faults and includes a series of deposits such as the Bouchard–Hébert Mine and possibly the Bousquet–Laronde deposits (outside the eastern limit in Fig. 10). This group is related to the annular faults of the Misema Caldera event, but associated with the Noranda Caldera event, in which 070° intersect the ring faults (Mueller et al., 2007). Numerous deposits are associated with carbonatization, such as the Bouchard–Hébert mine (Fig. 10). The Misema–New Senator–Noranda collapse calderas triggered the development of an interconnected fault pattern. Once initiated, this plumbing system could have driven hydrothermal fluids at various times, and peripheral Misema-related mineralization could thus be of different ages.

The megacaldera model provides an entirely new paradigm for exploration strategies. In this context, what was previously seen as loosely distributed and unrelated mineralizations become a tightly linked group related to synvolcanic fractures of the Misema collapse. Secondly, structures of the New Senator Caldera probably represent the main control on localizing mineralization, including the Horne deposit, six deposits in the immediate periphery of the McDougall–Despina fault system, and major showings and alteration zones on its southwest margin (e.g. Four-Corners, Yvanex and Innmont showing).

Current interpretations of carbonatization in the Archean Abitibi context preferentially point to a post-volcanic hydrothermal event intimately associated with “orogenic” gold mineralization. Although this is the case for structurally associated gold mineralization, Fig. 9 clearly indicates that carbonatization extends outside the classic structural corridors (i.e. Cadillac–Larder Lake and Destor–Porcupine). Altogether, carbonate distribution visibly mimics the ring fault pattern much more than the late structural corridors. This alteration is therefore interpreted as a Misema-related hydrothermal event.

6. Conclusions

New field observations of the Blake River Group and the reassessment of available information allow the proposition of an overlapping and nested megacaldera complex. Mafic dykes in the BRG present patterns that can be divided into two zones: external and internal ring and radial dyke swarms punctuated by local ovoid dyke swarms associated with volcanic centers. The overall dykes organization and the deduced stress field emphasizes the synvolcanic architecture. The combined features of the dyke pattern, the annular distribution of volcanoclastic deposits, the carbonate alteration zones at the BRG periphery, and the defined synvolcanic ring fault system are integrated into the evolution of the megacaldera complex.

The evolution of the megacaldera complex is described in five stages. Stage 1 corresponds to the development of a multi-vent mafic volcanic complex or shield volcano lying on a submarine plain. Stage 2 is associated with a first major collapse that created the giant Misema Caldera (80 km in diameter). A dyke swarm intruded synvolcanic fractures and an underlying magma chamber developed. Major volcanoclastic units were generated by local

volcanic centers spread out along the outer and inner ring faults that were used as conduits for CO₂-rich hydrothermal activity. Stage 3 represents renewed volcanic activity associated with a resurgent central dome inside the Misema Caldera. Stage 4 is the second collapse event that gave rise to the 35 km by 14 km NW-trending New Senator Caldera. This caldera was produced during a multi-step collapse following the SE migration of the underlying magmatic chamber, which later became the Flavrian–Powell Plutons. Stage 5 corresponds to the final collapse episode with the formation of the E–NE-trending Noranda Caldera that generated a well-developed 070°-trending fracture pattern associated with several VMS deposits.

Multiple caldera events provide an effective way to explain the presence of VMS mineralization along the synvolcanic fractures associated with the three collapse events, but the importance of the New Senator Caldera fracture pattern is emphasized for its role in the control of the giant Horne deposit. The geometry of the subaqueous BRG megacaldera compare favourably with modern subaerial counterparts such as the island-arc Taupo, the intra-continental Yellowstone, and the oceanic Hawaii and Canary Island calderas. The Blake River Caldera Complex is among the largest calderas on Earth and in this respect brings some new insights into Archean processes.

Acknowledgments

Valerio Acocella and Georges J. Hudak are especially thanked for their excellent reviews which have greatly improved the manuscript. Wulf Mueller provided his expertise in the review of several versions. This contribution presents several results from one project included in the CONSOREM’s research program. This study would not have been possible without the support of several people during data acquisition by the first author (Pearson). In alphabetical order, Ian Atkinson, Pierre Bertrand, Claude Britt, Jacqueline Gauthier, Harold Gibson, Gérald Riverin and Yvon Trudeau are especially thanked. CONSOREM’s company members and their representatives are also gratefully thanked for their cooperation during this project. This study was made in close collaboration with CONSOREM’s team, particularly Damien Gaboury, Stéphane Faure, Sylvain Trépanier and Hassan Nabil. Venetia Bodycomb and Isabelle Lapointe performed the initial editing and finally Claude Dallaire has worked on the illustrations.

References

- Acocella, V., 2007. Understanding caldera structure and development: an overview of analogue models compared to natural calderas. *Earth-Sci. Rev.* 85, 125–160.
- Acocella, V., Cifelli, F., Funicello, R., 2000. Analogue models of collapse calderas and resurgent domes. *J. Volcanol. Geotherm. Res.* 104, 81–96.
- Anderson, E.M., 1937. Cone sheets and rings dykes: the dynamical explanation. *Bull. Volcanol.* 1, 35–40.
- Annen, C., Lénat, J.-F., Provost, A., 2001. The long-term growth of volcanic edifices: numerical modelling of the role of dyke intrusion and lava-flow emplacement. *J. Volcanol. Geotherm. Res.* 105, 263–289.
- Ayer, J.A., Thurston, P.C., Bateman, R., Dubé, B., Gibson, H.L., Hamilton, M.A., Hathway, B., Hocker, S.M., Houllé, M.G., Hudak, G., Ispolatov, V.O., Lafrance, B., Leshner, C.M., MacDonald, P.J., Péloquin, A.S., Piercey, S.J., Reed, L.E., Thompson, P.H., 2005. Overview of results from the greenstone architecture project: discover Abitibi initiative. *Ont. Geol. Surv., Open File Report 6154*, 107 pp.
- Bachmann, O., Dungan, M.A., Lipman, P.W., 2002. The Fish canyon magma body, San Juan volcanic field, Colorado: rejuvenation and eruption of an upper-crustal batholith. *J. Petrol.* 43, 1469–1503.
- Baragar, W.R.A., 1968. Major-element geochemistry of the Noranda volcanic belt, Quebec–Ontario. *Can. J. Earth Sci.* 5, 773–790.
- Barrett, T.J., Cattalani, S., Hoy, L., Riopel, J., Lafleur, P.-J., 1992. Massive sulphide deposits of the Noranda area, Quebec. IV. The Mobrún Mine. *Can. J. Earth Sci.* 29, 1349–1374.
- Capdevilla, R., Goodwin, A.M., Ujike, O., Gorton, M.P., 1982. Trace-element geochemistry of Archean volcanic rocks and crustal growth in southwestern Abitibi belt, Canada. *Geology* 10, 418–422.

- Carracedo, J.C., 1994. The Canary Island: an example of structural control on the growth of large oceanic-island volcanoes. *J. Volcanol. Geotherm. Res.* 60, 225–241.
- Carracedo, J.C., Rodríguez Badiola, E., Guillou, H., Paterne, M., Scailliet, S., Pérez Torrado, F.J., Paris, R., Fra-Paleo, U., Hansen, A., 2007. Eruptive and structural history of Teide Volcano and rift zones of Tenerife, Canary Islands. *Geol. Soc. Am. Bull.* 119, 1027–1051.
- Cathles, L.M., 1993. Oxygen isotope alteration in the Noranda mining district, Abitibi greenstone belt, Quebec. *Econ. Geol.* 88, 1483–1511.
- Chesner, C.A., Rose, W.I., Deino, A., Drake, R., Westgate, J.A., 1991. Eruptive history of Earth's largest Quaternary caldera (Toba, Indonesia) clarified. *Geology* 19, 200–203.
- Charlier, B.L.A., Wilson, C.J.N., Lowenstern, J.B., Blake, S., van Calsteren, P.W., Davidson, J.P., 2005. Magma generation at a large, hyperactive silicic volcano (Taupo, New Zealand) revealed by U–Th and U–Pb systematics in zircons. *J. Petrol.* 46, 3–32.
- Chown, E.H., Daigneault, R., Mueller, W., Mortensen, J., 1992. Tectonic evolution of the Northern volcanic zone of the Abitibi belt. *Can. J. Earth Sci.* 29, 2211–2225.
- Christiansen, R.L., 1984. Yellowstone magmatic evolution: its bearing on understanding large-volume explosive volcanism. In: *Explosive Volcanism, Its Inception, Evolution and Hazards*. Nat. Res. Council Studies in Geophys., Nat. Acad. Press, Washington, DC, pp. 84–95.
- Christiansen, R.L., 1994. The Quaternary and Pliocene Yellowstone volcanic field of Wyoming, Idaho and Montana. *U.S. Geol. Surv. Prof. Pap.* 729-G.
- Clowes, R.M., Cook, F.A., Green, A.G., Keen, C.E., Ludden, J.N., Percival, J.A., Quinlan, G.M., West, G.F., 1992. Lithoprobe: new perspectives on crustal evolution. *Can. J. Earth Sci.* 29, 1813–1864.
- Cole, J.W., Milner, D.M., Spinks, K.D., 2005. Calderas and caldera structures: a review. *Earth-Sci. Rev.* 69, 1–26.
- Corfu, F., Noble, S.R., 1992. Genesis of the southern Abitibi greenstone belt, Superior Province, Canada; evidence from zircon Hf isotope analyses using a single filament technique. *Geochim. Cosmochim. Acta* 56, 2081–2097.
- Corfu, F., 1993. The evolution of the southern Abitibi greenstone belt in light of precise U–Pb geochronology. A special issue devoted to Abitibi ore deposits in a modern context. *Econ. Geol.* 88, 1323–1340.
- Corfu, F., Krogh, T.E., Kwok, Y.Y., Jensen, L.S., 1989. U–Pb zircon geochronology in the southwestern Abitibi greenstone belt, Superior Province. *Can. J. Earth Sci.* 26, 1747–1763.
- Daigneault, R., Archambault, G., 1990. Les grands couloirs de déformation de la sous-province de l'Abitibi. In: Rive, M., Riverin, G., Simard, A., Lulin, J.M., Gagnon, Y. (Eds.), *The Northwestern Quebec Polymetallic Belt: A Summary of 60 Years of Mining Exploration*, vol. 43. CIMM, Spec., pp. 43–64.
- Daigneault, R., Mueller, W., Chown, E.H., 2002. Oblique Archean subduction: accretion and exhumation of an oceanic arc during dextral transpression, Southern Volcanic Zone, Abitibi Subprovince Canada. *Precambrian Res.* 115, 261–290.
- Daigneault, R., Mueller, W.U., Chown, E.H., 2004. Abitibi greenstone belt plate tectonics: the diachronous history of arc development, accretion and collision. In: Eriksson, P.G., Altermann, W., Nelson, D.R., Mueller, W.U., Catuneanu, O. (Eds.), *The Precambrian Earth: Tempos and Events*, Series: *Developments in Precambrian geology*, vol. 12. Elsevier, pp. 88–103.
- David, J., Dion, C., Goutier, J., Roy, P., Bandyayera, D., Legault, M., Rhéaume, P., 2006. Datations U–Pb effectuées dans la Sous-province de l'Abitibi à la suite des travaux de 2004–2005, Ministère des Ressources naturelles et de la Faune du Québec, RP 2006-04, 22 pp.
- Davis, D.W., 2002. U–Pb geochronology of Archean metasedimentary rocks in the Pontiac and Abitibi subprovinces, Québec. *Precambrian Res.* 115, 97–117.
- Desgagné, J., 1995. Étude d'une brèche, la brèche Gabriel, dans un contexte volcanosédimentaire. Ben Nevis, Ontario, Canada. B.Sc. Thesis. Univ. du Québec à Chicoutimi, 50 pp.
- de Rosen-Spence, A.F., 1976. Stratigraphy, development, and petrogenesis of the Noranda volcanic pile, Noranda, Quebec. Ph.D. Thesis. Univ. Toronto, Toronto, Ont., 116 pp.
- Dieterich, J.H., 1988. Growth and persistence of Hawaiian volcanic rift zones. *J. Geophys. Res.* 93 (B5), 4258–4270.
- Dimroth, E., Desmarke, J., 1978. Petrography and mechanism of eruption of the d'Alembert tuff, Rouyn-Noranda, Quebec, Canada. *Can. J. Earth Sci.* 15, 1712–1723.
- Dimroth, E., Lichtblau, A.P., 1979. Metamorphic evolution of Archean hyaloclastites, Noranda area, Quebec, Canada. Part I. Comparison of Archean and Cenozoic seafloor metamorphism. *Can. J. Earth Sci.* 16, 1315–1340.
- Dimroth, E., Imreh, L., Cousineau, P., Leduc, M., Sanschagrin, Y., 1985. Paeogeographic analysis of mafic submarine flows and its use in the exploration for massive sulphide deposits. In: Ayres, L.D., Thurston, P.C., Card, K.D., Weber, W. (Eds.), *Evolution of Archean Supracrustal Sequences*, *Geol. Ass. Can., Spec. Pap.*, vol. 28, pp. 203–222.
- Dimroth, E., Imreh, L., Goulet, N., Rocheleau, M., 1983. Evolution of the south-central part of the Archean Abitibi Belt, Quebec. Part II. Tectonic evolution and geomechanical model. *Can. J. Earth Sci.* 20, 1355–1373.
- Dimroth, E., Imreh, L., Rocheleau, M., Goulet, N., 1982. Evolution of the south-central part of the Archean Abitibi Belt, Quebec. Part I. Stratigraphy and paleogeographic model. *Can. J. Earth Sci.* 19, 1729–1758.
- Dimroth, E., Rocheleau, M., 1979. Volcanologie et sédimentologie, dans la région de Rouyn-Noranda, Québec. GAC-MAC Annual Meeting, Excursion A-1, 212 pp.
- Dion, C., Legault, M., 2005. Potential of the Blake River Group. Québec Exploration 2005. Abstracts of oral presentations and posters. Interactive sessions. Ass. Explor. Min. Qué. and Min. Ress. Nat. et Faune Québec. Join meeting. Château Frontenac, Québec, p. 107.
- Ernst, R.E., Head, J.W., Parfitt, E., Grosfils, E., Wilson, L., 1995. Giant radiating dyke swarms on Earth and Venus. *Earth-Sci. Rev.* 39, 1–58.
- Fiske, R.S., Jackson, E.D., 1972. Orientation and growth of Hawaiian volcanic rifts: the effect of regional structure and gravitational stresses. *Proc. R. Soc. Lond.* 329, 299–326.
- Fiske, R.S., Naka, J., Iizasa, K., Yuasa, M., Klaus, A., 2001. Submarine silicic caldera at the front of the Izu-Bonin Arc, Japan: voluminous seafloor eruptions of rhyolite pumice. *Geol. Soc. Am. Bull.* 113, 813–824.
- Fiske, R.S., Cashman, C.V., Shibata, A., Watanabe, K., 1998. Tephra dispersal from Myojinsho, Japan, during its shallow submarine eruption of 1952–1953. *Bull. Volcanol.* 59, 262–275.
- Franklin, J.M., Gibson, H.L., Jonasson, I.R., Galley, A.G., 2005. Volcanogenic Massive Sulfide Deposits. In: Hedenquist, J.W., Thompson, J.F.H., Goldfarb, R.J., Richards, J.P. (Eds.), *Econ. Geology and the Bull. of the Soc. of Econ. Geol., One Hundredth Anniversary Volume 1905–2005*, pp. 523–560.
- Fowler, A.D., Jensen, L.S., 1989. Quantitative trace-element modelling of the crystallization of the Kinjovis and Blake River Groups, Abitibi greenstone belt, Ontario. *Can. J. Earth Sci.* 26, 1356–1367.
- Gagnon, M., Mueller, W., Riverin, G., 1995. Volcanic construction of an Archean upwards shoaling sequence: the Ben Nevis volcanic complex, Ontario, Precambrian 95. In: *International Conference on Tectonic & Metallogeny of Early/Mid Precambrian Orogenic Belts, Program and Abstracts*, vol. 81, Montréal.
- Galley, A.G., van Breemen, O., 2002. Timing of Synvolcanic Magmatism in Relation to Base-metal Mineralization, Rouyn-Noranda, Abitibi Volcanic Belt, Québec. *Current Research 2002-F8*. Geological Survey of Canada, p. 9.
- Gélinas, L., Ludden, J.N., 1984. Rhyolitic volcanism and the geochemical evolution of an Archean central ring complex: the Blake River Group volcanics of the southern Abitibi belt, Superior province. *Phys. Earth Planet. Inter.* 35, 77–88.
- Gélinas, L., Brooks, C., Perrault, G., Carignan, J., Trudel, P., Grasso, F., 1977. Chemostratigraphic division within the Abitibi volcanic belt, Rouyn-Noranda district, Quebec. In: Baragar, W.R.A., Coleman, L.C., Hall, J.M. (Eds.), *Volcanic Regimes in Canada*, *Geol. Ass. Can., Spec. Pap.*, vol. 16, pp. 265–295.
- Gélinas, L., Trudel, P., Hubert, C., 1984. Chemostratigraphic division of the Blake River Group, Rouyn-Noranda area, Abitibi, Québec. *Can. J. Earth Sci.* 21, 220–231.
- Gibson, H.L., 1989. The mine sequence of the central Noranda volcanic complex: geology, alteration, massive sulphide deposits and volcanological reconstruction. Ph.D. Thesis. Carleton Univ., Ottawa, Ont., 715 pp.
- Gibson, H.L., Morton, R.L., Hudak, G.L., 1999. Submarine volcanic processes, deposits and environments favourable for the location of volcanic-associated massive sulphide deposits. In: Barrie, C.T., Hannington, M.D. (Eds.), *Volcanic Associated Massive Sulfide Deposits: Processes and Examples in Modern and Ancient Settings*. *Review in Econ. Geology*, vol. 8, pp. 13–51.
- Gibson, H.L., Watkinson, D.H., 1990. Volcanogenic massive sulphide deposits of the Noranda cauldron and shield volcano, Quebec. In: Rive, M., Verpaest, P., Gagnon, Y., Lulin, J.-M., Riverin, G., Simard, A. (Eds.), *The Northwestern Quebec Polymetallic Belt: A Summary of 60 Years of Mining Exploration*. *Can. Inst. Min. Metal., Spec.*, vol. 43, pp. 119–132.
- Goff, F., Gardner, J.N., Baldrige, W.S., Hulen, J.B., Nielson, D.L., Vaniman, D., Heiken, G., Dungan, M.A., Broxton, D., 1989. Excursion 17B: Volcanic and Hydrothermal Evolution of Valles Caldera and Jemez Volcanic field. *New Mexico Bureau of Mines and Mineral Resources, Memoir*, p. 46.
- Goldie, R., 1979. Consanguineous Archean intrusive and extrusive rocks, Noranda, Quebec: chemical similarities and differences. *Precambrian Res.* 9, 275–287.
- Goodwin, A.M., 1965. Mineralized volcanic complexes in the Porcupine, -Kirkland Lake-Noranda region, Canada. *Econ. Geol.* 60, 955–971.
- Goodwin, A.M., 1977. Archean volcanism in Superior Province, Canadian shield. In: Baragar, W.R.A., Coleman, L.C., Hall, J.M. (Eds.), *Volcanic Regimes in Canada*, *Geol. Ass. Can., Spec. Pap.*, vol. 16, pp. 205–241.
- Goodwin, A.M., 1979. Archean volcanic studies in the Timmins-Kirkland lake-Noranda region of Ontario and Quebec. *Geol. Surv. Can., Bull.* 278, 51.
- Goodwin, A.M., 1982. Archean volcanoes in southwestern Abitibi belt, Ontario and Quebec: form, composition, and development. *Can. J. Earth Sci.* 19, 1140–1155.
- Goodwin, A.M., Smith, I.E.M., 1980. Chemical discontinuities in Archean volcanic terrains and the development of Archean crust. *Precambrian Res.* 10, 301–311.
- Goodwin, A.M., Ridler, R.H., 1970. The Abitibi orogenic belt. In: *Basins and geosynclines of the Canadian shield*, vol. 70–40. Geological Survey of Canada, pp. 1–30.
- Goutier, J., 1997. Géologie de la région de Destor, Québec. *Min. Res. Nat. Qué., Rap. Géol. RG 96-13*, p. 37.
- Goutier, J., Melançon, M., 2007. Compilation géologique de la Sous-province de l'Abitibi (version préliminaire). Ministère des Ressources naturelles et de la Faune, Québec; échelle 1/500 000.
- Gray, J.P., Monaghan, J.J., 2004. Numerical modelling of stress fields and fracture around magma chambers. *J. Volcanol. Geotherm. Res.* 135, 259–283.
- Green, A.G., Mayrand, L.J., Milkeriet, B., Ludden, J.N., Hubert, C., Jackson, S.L., Sutcliffe, R.H., West, G.F., Verpaest, P., Simard, A., 1990. Deep structure of an Archean greenstone terrane. *Nature* 344, 327–330.
- Grunsky, E.C., 1986. Recognition of alteration in volcanic rocks using statistical analysis of lithochemical data. In: Wood, J., Wallace, H. (Eds.), *Volcanology and Mineral Deposits*, *Ont. Geol. Surv., Misc. Pap.*, vol. 129, pp. 124–173.
- Gudmundsson, A., 2002. Emplacement and arrest of sheets and dykes in central volcanoes. *J. Volcanol. Geotherm. Res.* 116, 279–298.

- Gudmundsson, A., 1998a. Magma chambers modeled as cavities explain the formation of rift zone central volcanoes and their eruption and intrusion statistics. *J. Geophys. Res.* 103, 7401–7412.
- Gudmundsson, A., 1998b. Formation and development of normal-fault calderas and the initiation of large explosive eruptions. *Bull. Volcanol.* 60, 160–171.
- Gudmundsson, A., Marinoni, L.B., Marti, J., 1999. Injection and arrest of dykes: implications for volcanic hazards. *J. Volcanol. Geotherm. Res.* 88, 1–13.
- Gudmundsson, A., Marti, J., Turon, E., 1997. Stress fields generation ring faults in volcanoes. *Geophys. Res. Lett.* 24, 1559–1562.
- Hannington, M.D., Santaguida, F., Kjarsgaard, I.M., Cathles, L.M., 2003. Regional-scale hydrothermal alteration in the central Blake River Group, western Abitibi, Canada: implications for VMS prospectivity. *Mineral. Deposita* 38, 393–422.
- Hart, T.R., Gibson, H.L., Leshar, C.M., 2004. Trace element geochemistry and petrogenesis of felsic volcanic rocks associated with volcanogenic massive Cu–Zn–Pb sulfide deposits. *Econ. Geol.* 99, 1003–1013.
- Hogg, W.A., 1964. Arnold and Katrine townships, Ont. Dept. Mines, Geol. Rep., vol. 29, p. 15.
- Hudak, G.J., Morton, R.L., Franklin, J.M., Paterson, D.M., 2003. Morphology, distribution and estimated eruption volumes for intracaldera tuffs associated with volcanic-hosted massive sulphide deposits in the Archean Sturgeon Lake caldera complex, Northwestern Ontario. In: White, J.D.L., Smellie, J.L., Clague, D.A. (Eds.), *Explosive Subaqueous Volcanism*. Am. Geophys. Union, Geophys. Monogr., vol. 140, pp. 345–360.
- Jackson, S.L., Sutcliffe, R.H., Ludden, J.N., Hubert, C., Green, A.G., Milkereit, B., Mayrand, L., West, G.F., Verpaest, P., 1990. Southern Abitibi greenstone belt: Archean crustal structure from seismic-reflection profiles. *Geology* 18, 1086–1090.
- Jensen, L.S., 2005. Geology of Thackeray, Elliott, Tannahill and Dokis townships, district of Cochrane, Ont. Div. Mines, Min. Nat. Res., Geosc. Rep., vol. 165, 71 pp.
- Jensen, L.S., 1981. A petrogenic model for the Archean Abitibi Belt in the Kirkland Lake area, Ontario. Ph.D. Thesis. University of Saskatchewan, Saskatchewan, 421 pp.
- Jolly, W.T., 1978. Metamorphic history of the Archean Abitibi belt, Metamorphism on the Canadian shield, *Geol. Surv. Can.*, Paper 78–10, pp. 63–78.
- Jolly, W.T., 1980. Development and degradation of Archean lavas, Abitibi area, Canada, in light of major element geochemistry. *J. Petrol.* 21, 323–363.
- Kennedy, P.K., 1984. The geology and geochemistry of the Archean Flawlin pluton, Noranda, Quebec. Ph.D. Thesis. Univ. Western Ontario, London, Ontario, 469 pp.
- Kerr, D.J., Mason, R., 1990. A re-appraisal of the geology and ore deposits of the Horne mine complex at Rouyn-Noranda, Quebec. In: Rive, M., Verpaest, P., Gagnon, Y., Lulin, J.-M., Riverin, G., Simard, A. (Eds.), *The Northwestern Quebec Polymetallic Belt: A Summary of 60 Years of Mining Exploration*, Can. Inst. Min. Metal., Spec., vol. 43, pp. 153–165.
- Kissling, W.M., Weir, G.J., 2005. The spatial distribution of the geothermal fields in the Taupo volcanic zone, New Zealand. *J. Volcanol. Geotherm. Res.* 145, 136–150.
- Knuckey, M.J., Comba, C.D.A., Riverin, G., 1982. Structure, metal zoning and alteration at the Millenbach deposit, Noranda, Quebec. In: Hutchinson, R.W., Spence, C.D., Franklin, J.M. (Eds.), *Precambrian Sulphide Deposits*, Geol. Ass. Can., Spec. Pap., vol. 25, pp. 255–294.
- Lafleche, M.R., Dupuy, C., Dostal, J., 1992. Tholeiitic volcanic rocks of the Late Archean Blake River Group, southern Abitibi greenstone belt: origin and geodynamic implications. *Can. J. Earth Sci.* 29, 1448–1458.
- Lafrance, B., 2003. Reconstruction d'un environnement de sulfures massifs volcanogènes déformés: exemple archéen de Normétal, Abitibi. Ph.D. Thesis. Université du Québec à Chicoutimi, Canada (<http://theses.uqac.ca/>), 362 pp.
- Lafrance, B., Davis, D.W., Goutier, J., Moorhead, J., Pilote, P., Mercier-Langevin, P., Dubé, B., Galley, A.G., Mueller, W.U., 2005. Nouvelles datations isotopiques dans la portion québécoise du Groupe de Blake River et des unités adjacentes, Min. Ener. Ress. Faune et Parc. RP 2005-01, 15 pp.
- Lafrance, B., Moorhead, J., Davis, D.W., Cadre géologique du camp minier de Doyon-Bousquet-LaRonde, Québec. Min. Res. Nat. Qué. ET 2002-07, 43 pp.
- Lafrance, B., Mueller, W.U., Daigneault, R., Dupras, N., 2000. Evolution of a submergéd composite arc volcano: volcanology and geochemistry of the Normetal volcanic complex, Abitibi greenstone belt, Quebec, Canada. *Precambrian Res.* 101, 277–311.
- Lichtblau, A., Dimroth, E., 1980. Stratigraphy and facies at the south margin of the Archean Noranda caldera, Noranda, Québec. *Current Research, Part A, Geological Survey of Canada*, Paper 80-1A, pp. 69–76.
- Lipman, P.W., 1997. Subsidence of ash-flow calderas: relation to caldera size and magma-chamber geometry. *Bull. Volcanol.* 59, 198–218.
- Ludden, J.N., Pélouin, S.A., 1996. A geodynamic model for the evolution of the Abitibi Belt; implications for the origins of volcanic massive sulphide (VMS) deposits. *Trace Element Geochemistry of Volcanic Rocks; Applications For Massive Sulphide Exploration*, Short Course Notes, Geological Association of Canada, vol. 12, pp. 205–237.
- Ludden, J.N., Gélinas, L., Trudel, P., 1982. Archean metavolcanics from the Rouyn-Noranda district, Abitibi greenstone belt, Québec: mobility of trace elements and petrogenetic constraints. *Can. J. Earth Sci.* 19, 2276–2287.
- Ludden, J.N., Hubert, C., Barnes, A., Milkereit, B., Sawyer, E., 1993. A three dimensional perspective on the evolution of Archean crust: LITHOPROBE seismic reflection images in the southwestern Superior province. *Lithos* 30, 357–372.
- Marti, J., Gudmundsson, A., 2000. The Las Canadas caldera (Tenerife, Canary islands): an overlapping collapse caldera generated by magma-chamber migration. *J. Volcanol. Geotherm. Res.* 103, 161–173.
- Marinoni, L.B., Gudmundsson, A., 2000. Dykes, faults and palaeostresses in the Teno and Anaga massifs of Tenerife (Canary Islands). *The geology and geophysics of Tenerife*. *J. Volcanol. Geotherm. Res.* 103, 83–103.
- Martin, L., Masson, M., 2005. Towards new discoveries thanks to the application of 3D modeling in the Noranda camp. Québec Exploration 2005. Abstracts of oral presentations and posters. Ass. Explor. Min. Qué. and Min. Ress. Nat. et Faune Qué. Join meeting, Château Frontenac, Québec, p. 88.
- Masson, M., 2005. Recent exploration success stories in the Noranda mining camp. Québec Exploration 2005. Abstracts of oral presentations and posters. Ass. Explor. Min. Qué. and Min. Ress. Nat. et Faune Qué. Join meeting, Château Frontenac, Québec, p. 72.
- McGuire, W.J., Pullen, A.D., 1989. Location and orientation of eruptive fissures and feeder-dykes at Mount Etna; influence of gravitational and regional tectonic stress regimes. *J. Volcanol. Geotherm. Res.* 38, 325–344.
- Mortensen, J.K., 1993a. U–Pb geochronology of the eastern Abitibi Subprovince. Part 1. Chibougamau-Matagami-Joutel region. *Can. J. Earth Sci.* 30, 11–28.
- Mortensen, J.K., 1993b. U–Pb geochronology of the eastern Abitibi subprovince. Part 2. Noranda-Kirkland lake area. *Can. J. Earth Sci.* 30, 29–41.
- Morton, R.L., Franklin, J.M., 1987. Two-fold classification of Archean volcanic-associated massive sulfide deposits. *Econ. Geol.* 82, 1057–1063.
- Morton, R.L., Walker, J.S., Hudak, G.J., Franklin, J.M., 1991. The early development of an Archean submarine caldera complex with emphasis on the Mattabi ash-flow tuff and its relationship to the Mattabi massive sulfide deposit. *Econ. Geol.* 86, 1002–1011.
- MRNFP, 2005. Carte des gîtes minéraux, 1:50 000, 32D06 – Rivière Kanasuta. Carte SI-32D06-G3P-05F, Min. Ress. Nat. et de la Faune, Québec.
- Mueller, W., White, J.D.L., 1992. Felsic fire-fountaining beneath Archean seas: pyroclastic deposits of the 2730 MA Hunter Mine Group, Quebec, Canada. *J. Volcanol. Geotherm. Res.* 54, 117–134.
- Mueller, W.U., Stix, J., White, J.D.L., Hudak, G., 2004. Archean calderas. In: Eriksson, P., Altermann, W., Nelson, D., Mueller, W.U., Cataneanu, O. (Eds.), *The Precambrian Earth: tempos and events in Developments in Precambrian Geology*, vol. 12. Elsevier, pp. 345–356.
- Mueller, W.U., Stix, J., White, J.D.L., Corcoran, P.L., Lafrance, B., Daigneault, R., 2008. Characterization of Archean subaqueous calderas in Canada: physical volcanology, carbonate-rich hydrothermal alteration and new exploration model. In: Gottsmann, J., Marti, J. (Eds.), *Caldera Volcanoes: Analysis, Modeling and Response*. *Developments in Volcanology*, vol. 10. Elsevier, pp. 183–232 (Chapter 5).
- Mueller, W.U., Pearson, V., Mortensen, J.K., 2007. Évolution sous-marine du Groupe de Blake River: Nouvelles datation et caractéristiques des caldeiras Archéennes de Misema et de New Senator. *Recueil des résumés, Carrefour des Science de la Terre, Univ. Québec à Chicoutimi*, p. 45.
- Mueller, W.U., Mortensen, J.K., 2002. Age constraints and characteristics of subaqueous volcanic construction, the Archean Hunter Mine Group, Abitibi greenstone belt. *Precambrian Res.* 115, 119–152.
- Nabil, H., 2007. *Projet 2006-04, Zonalité et typologie de la carbonatation pour les minéralisations aurifères et métaux de bases volcanogènes – Phase 2, CON-SOREM*. Unpublished Internal report, 34 pp.
- Nakamura, K., 1977. Volcanoes as possible indicators of tectonic stress orientation—principle and proposal. *J. Volcanol. Geotherm. Res.* 2, 1–16.
- Nunes, P.D., Jensen, L.S., 1980. Geochronology of the Abitibi metavolcanic belt, Kirkland Lake area; progress report. *Summary of Geochronology Studies; 1977–1979*, Ontario Geological Survey Miscellaneous Paper no. 92, pp. 40–45.
- Ohmoto, H., 1996. Formation of volcanogenic massive sulfide deposits: the Kuroko perspective. *Ore Geol. Rev.* 10, 135–177.
- Ohmoto, H., 1978. Submarine calderas: a key to the formation of volcanogenic massive sulfide deposits. *Min. Geol.* 89, 1687–1696.
- Paradis, S., Ludden, J., Gélinas, L., 1988. Evidence for contrasting compositional spectra in comagmatic intrusive and extrusive rocks of the late Archean Blake River Group, Abitibi, Quebec. *Can. J. Earth Sci.* 25, 134–144.
- Pearson, V., 1986. *Pétrographie, géochimie et interprétation d'un assemblage à cordiérite-anthophyllite dans les roches mafiques Archéennes de Macanda, canton Beauchastel, Noranda, Québec*. M.Sc. Thesis. Univ. Québec Chicoutimi, 168 pp.
- Pearson, V., 1994. Ben-Nevis: 1992–1994 synthesis, integration of geological, litho-geochemical and geophysical data. Unpublished Internal report, Metall Mining Corporation, 35 pp.
- Pearson, V., 1994. *Propriété Flag: Synthèse 1989–1994*. Unpublished internal report, Metall Mining Corporation, 147 pp.
- Pélouin, S.A., 2000. Reappraisal of the Blake River Group stratigraphy and its place in the Archean volcanic record, Ph.D. Thesis. Université de Montréal, Montréal, QC, Canada, 282 pp.
- Pilote, C., Mueller, W., Perron, M., Les dépôts pyroclastiques sous-marins de la caldera de Misema, Groupe de Blake River. *Abstract. Carrefour des Sciences de la Terre, Univ. Québec à Chicoutimi*, p. 38.
- Price, P., 1948. Horne Mine. In: Graham, R.P.D. Ed., *Structural Geology of Canadian Ore Deposits*, Can. Inst. Min. Metal., Jubilee 1, pp. 763–772.
- Roche, O., Druitt, T.H., Merle, O., 2000. Experimental study of caldera formation. *J. Geophys. Res.* 105, 395–416.
- Ross, P.-S., Percival, J.A., Mercier-Langevin, P., Goutier, J., McNicoll, V.J., Dubé, B., 2007. Intermediate to mafic volcanoclastic units in the peripheral Blake River Group, Abitibi Greenstone Belt, Quebec: origin and implications for volcanogenic massive sulphide exploration. *Geol. Surv. Can., Current Research 2007-C3*, 25 pp.

- Ryan, M.P., 1988. The mechanics and three-dimensional structure of active magmatic system: Kilauea volcano, Hawaii. *J. Geophys. Res.* 93 (B5), 4213–4248.
- Santaguida, F., 1999. The paragenetic relationships of epidote-quartz hydrothermal alteration within the Noranda volcanic complex, Quebec. Ph.D. Thesis. Carleton Univ., Ottawa, 302 pp.
- Self, S., Heiken, G., Sykes, M.L., Wolertz, K., Fisher, R.V., Dethier, D.P., 1996. Field excursions to the Jemez Mountains, New Mexico. *N. Mex. Bureau Mines Miner. Resour. Bull.* 134, 72.
- Setterfield, T., 1987. Massive and brecciated dikes in the McDougall and Despina faults, Noranda, Quebec, Canada. *J. Volcanol. Geotherm. Res.* 31, 87–97.
- Setterfield, T.N., Hodder, R.W., Gibson, H.L., Watkins, J.J., 1995. The McDougall–Despina fault set, Quebec: evidence for fault-controlled volcanism and hydrothermal fluid flow. *Explor. Min. Geol.* 4, 381–393.
- Scott, S.D., 1980. Geology and structural control of Kuroko-type massive sulphide deposits. In: Strangway, D.W. (Ed.), *The Continental Crust and Its Mineral Deposits*. Geol. Ass. Can., Spec. Pap., vol. 20, pp. 705–722.
- Smith, R.P. 1987. Dyke emplacement at Spanish Peaks, Colorado. In: Halls, H.C., Fahrig, W.F. (Eds.), *Mafic Dyke Swarms*. Geol. Ass. Can., Spec. Pap., vol. 34, pp. 47–54.
- Stix, J., Kennedy, B., Hannington, M., Gibson, H., Fiske, R., Mueller, W., Franklin, J., 2003. Caldera-forming processes and the origin of submarine volcanogenic massive sulfide deposits. *Geology* 31, 375–378.
- Takada, A., 1999. Variations in magma supply and magma partitioning: the role of tectonic settings. *J. Volcanol. Geotherm. Res.* 93, 93–110.
- Tassé, N., Lajoie, J., Dimroth, E., 1978. The anatomy and interpretation of an Archean volcanoclastic sequence, Noranda region, Québec. *Can. J. Earth Sci.* 15, 874–888.
- Tibaldi, A., 2003. Influence of cone morphology on dykes, Stromboli, Italy. *J. Volcanol. Geotherm. Res.* 126, 79–95.
- Ujike, O., Goodwin, A.M., 1987. Geochemistry and origin of Archean metavolcanic rocks, central Noranda area, Québec, Canada. *Can. J. Earth Sci.* 24, 2551–2567.
- Vaillancourt, D., 1996. Âges U-Pb des minéralisations de type sulfures massifs volcanogènes dans le Groupe de Blake River de la Sous-Province de l'Abitibi, Québec: Les sites d'Aldermac, Hébécourt et Millenbach., Université du Québec à Montréal, 32 pp.
- Walker, G.P.L., 1999. Volcanic rift zones and their intrusion swarms. *J. Volcanol. Geotherm. Res.* 94, 21–34.
- Walter, T.R., Troll, V.R., 2001. Formation of caldera periphery faults: an experimental study. *Bull. Volcanol.* 63, 191–203.
- Walter, T.R., Troll, V.R., 2003. Experiments on rift zone evolution in unstable volcanic edifices. *J. Volcanol. Geotherm. Res.* 127, 107–120.
- Wilson, C.J.N., Blake, S., Charlier, B.L.A., Sutton, A.N., 2006. The 26.5 ka Oruanui eruption, Taupo volcano, New Zealand: development, characteristics and evacuation of a large rhyolitic magma body. *J. Petrol.* 47, 35–69.